Research on
Engineering
Structures & Materials
journal homepage: http://jresm.org

RESEARCH
GROUP

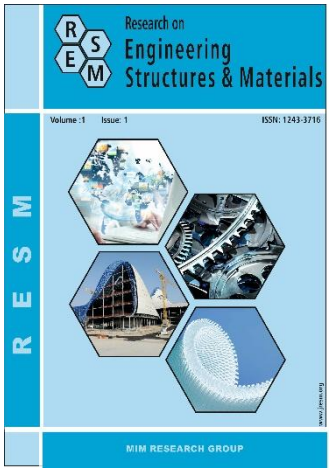

Finite element analysis of transient thermal performance of a convective-radiative cooling fin: effects of fin tip conditions and magnetic field

M. G. Sobamowo

Online Publication Date: 25 Oct 2018
URL: http://dx.doi.org/10.17515/resm2018.52me0526
DOI: http://dx.doi.org/10.17515/resm2018.52me0526

Journal Abbreviation: *Res. Eng. Struct. Mat.*

To cite this article
Sobamowo MG. Finite element analysis of transient thermal performance of a convective-radiative cooling fin: effects of fin tip conditions and magnetic field. *Res. Eng. Struct. Mat.*, 2019; 5(1): 43-74.

Research on Engineering Structures & Materials
journal homepage: http://jresm.org
Research Group

Research Article

Finite element analysis of transient thermal performance of a convective-radiative cooling fin: effects of fin tip conditions and magnetic field

M. G. Sobamowo[a]

Department of Mechanical Engineering, University of Lagos, Akoka, Lagos, Nigeria.

Article Info

Article history:
Received 25 Jun 2018
Revised 02 Oct 2018
Accepted 25 Oct 2018

Keywords:
Transient analysis;
Fin tip conditions;
Finite element method;
Magnetic field;

Abstract

The wide range of applications of cooling fins are evident in heat transfer enhancements for various thermal systems and also, for the control and prevention of thermal damages in mechanical and electronic equipment. In this work, nonlinear thermal behaviour of convective-radiative cooling fin with convective tip and subjected to magnetic field is analyzed using Galerkin finite element method. The numerical solutions are verified by the exact analytical solution of the linearized models using Laplace transforms method. Based on the numerical investigations, it is established that increase in Biot number, convective, radiative and magnetic parameters increase the rate of heat transfer from the fin and consequently improve the efficiency of the cooling fin. Also, the study shows that for a relatively short cooling fin operating for prolonged periods of time or steady state, the adiabatic/hypothetical condition (or negligible heat transfer) at the tip can be assumed without any significant loss in accuracy or equality as compared to the convective condition at the tip. However, for a long cooling fin of finite length operating in a transient state, especially for short period of time, the assumption of insulated tip produces significant different results as compared to the results of the convective tip. Therefore, for transient thermal studies of fins, the assumption that no heat transfer takes place at the fin tip should be taken with caution for a long cooling fin of finite length operating within a relatively short period of time. It is hope that the present study will enhance the understanding of transient thermal response of the solid fin under various factors and fin tip conditions.

1. Introduction

The increasing demands for high performance thermal equipment require the development of enhanced heat transfer devices. Also, the generation of excessive heat that leads to thermal-induced failure in various thermal systems calls for the production of effective heat dissipating devices that will enhance the rate of heat transfer from the thermal equipment. In order to meet these needs, extended surfaces such as fins and spines have been applied in various thermal and electronic equipment. Consequently, the applications of the extended surfaces in the thermal systems such as air conditioning, refrigeration, super heaters, automobile, power plants, heat exchangers, convectional furnaces, economizers, gas turbines, chemical processing equipment, oil carrying pipelines, computer processors, electrical chips, electronic and microelectronics components, high-power semi-conductor devices, high-power lasers, light emitting diodes (LEDs), computer cooling, sensitive devices etc. have attracted various research interests in few past decades. The thermal analysis of the extended surfaces involves the development of thermal models for various operating conditions. Different analytical

*Corresponding author: mikegbeminiyi@gmail.com
[a]orcid.org/0000-0003-2402-1423
DOI: http://dx.doi.org/10.17515/resm2018.52me0526

(exact and approximate) and numerical methods have been employed by various researchers to analyze the developed thermal models of the extended surfaces. Exact analytical methods such as methods of superposition and separation of variables were employed by Wang *et al.* [1] while Moitsheki and Harley [2], Mhlongo and Moitsheki [3], Ali *et al.* [4] and Kader *et al.* [5] adopted Lie point symmetry method for the thermal analysis of fins. Kirchoff's transformation method was adopted by Moitsheki and Rowjee [6]. In an earlier work, Cole *et al*. [7] made use of Green's functions (GF) in the form of infinite series to present analytical solutions to the differential equations governing the thermal behaviour of fins.

The above reviewed works provided exact analytical solutions to the thermal models governing the thermal behaviours of the fins under various operating conditions. However, most of the developed exact analytical solutions are based on the assumptions of constant thermal properties. Indubitably, the idealization of a constant or uniform heat transfer coefficient is not realistic. This is because in practice, heat transfer coefficients has significantly greater values at the fin tip more than the fin base. Additionally, the heat transfer coefficients vary with temperature. Such variation of the heat transfer coefficient as a function of temperature is often governed by a power law. Moreover, the thermal conductivity of the fin is temperature-dependent. Under these circumstances, the differential equations governing the thermal responses of the fin under various conditions become strictly nonlinear. Therefore, large numbers of the past studies have applied various approximate analytical methods to solve the nonlinear thermal models under various geometrical, internal and external conditions. In past few decades, Jordan et al. [8] utilized optimal linearization method while Kundu and Das [9] adopted Frobenius expanding series for the nonlinear fin problems. Homotopy analysis method was used by Khani et al. [10] and Amirkolaei and Ganji [11]. Aziz and Bouaziz [12] employed method of least squares while Sobamowo [13], Ganji et al. [14] and Sobamowo et al. [15] applied Galerkin method of weighted residual to analyze the thermal behaviour of the extended surfaces. In recent times, double decomposition and variation of parameter methods were employed by Sobamowo [16] and Sobamowo et al. [17], respectively to investigate the heat transfer characteristics of fins. In some other works, Moradi and Ahmadikia [18], Sadri et al. [19], Ndlovu and Moitsheki [20], Mosayebidarchech et al. [21], Ghasemi et al. [22] and Ganji and Dogonchi [23] adopted differential transformation method to determine the temperature distribution in fins. Applications of homotopy perturbation method to the fin problem was presented by Sobamowo et al. [24], Arslanturk [25], Ganji et al. [26] and Hoshyar et al. [27].

The developed series solutions for the thermal analyses of fins using different approximate analytical methods involve large number of terms. In practice, such expressions involving large number of terms are not convenient for use by designers and engineers [13]. Therefore, over the years, various numerical methods have been explored to analyze the thermal behavior of various extended surfaces. In an earlier work on numerical analysis of determination of temperature distribution in fins, Singh *et al.* [28] adopted meshless element free Galerkin method. Few years later, Basri *et al.* [29] presented a study on the applications of efficient finite element and differential quadrature methods to the heat transfer problems. Singh *et al.* [30] and Sao and Banjare [31] used quasi- steady theory while in the same year, Lotfi and Belkacem [32] and Al- Rashed *et al.* [33] utilized finite volume method for the thermal analysis of fins. In another study, Taler and Taler [34] presented the coupling of finite volume finite element methods to the heat transfer problem. Incremented differential quadrature method was used by Malekzadeh and Rahideh [35]. Reddy et al. [36] adopted B- spline based finite element method while Sun et al. [37] applied collocation spectral method to the fin problem. Rajul et al. [38] examined the thermal response of the fin using Meshless Local Petrov-Galerkin (MLPG). In the

preceding year, Wei *et al.* [39] investigated the thermal behaviour of fin through field synergy principle optimization analysis. Hajabdollahi et al. [40] presented genetic algorithm while symbolic programming was used by Fatoorehchi and Abolghasemi [41]. Three years later, Latif *et al.* [42] successfully applied symmetry reduction method to address nonlinear heat transfer problems of fins. In the same year, Mahmoudi and Mejri [43] used to Lattice Boltzmann method to investigate the effect of variable thermal conductivity and variable refractive index on transient conduction and radiation heat transfer. In some recent studies, Sobamowo [44] and Sobamowo et al. [45] applied finite difference and finite volume method, respectively for thermal analysis of longitudinal fin with temperature-dependent thermal conductivity and internal heat generation. Also, Sobamowo et al. [46] and Sobamowo [47] adopted Legendre wavelet collocation method to investigate the effects of magnetic field on the thermal performance of convective-radiative fin and also to study heat transfer in porous fin with temperature-dependent thermal conductivity and internal heat generation. Sobamowo and Kamiyo [48] studied multi-boiling heat transfer behavior of a convective straight fin with temperature-dependent thermal properties and internal heat generation using finite volume method. In another study, Chebychev spectral collocation method was used by Sobamowo [49] to examine the heat transfer in porous fin with temperature-dependent thermal conductivity and internal heat generation.

It should be noted that most of the above reviewed studies are based on steady state analysis of fin. However, in many engineering practices and devices such as in automobiles, study of heat transfer in building, industrial applications, transient analysis is very important. In fact, an accurate transient analysis provides insight into the design of fins that would fail in steady-state operations but are sufficient for desired operating periods. Consequently, there have been comparatively few studies on the transient analysis of the fin. In some earlier works, transient closed form solutions were developed for fin with assumed constant thermal properties. Chapman [50] studied the transient behavior of an annular fin of uniform thickness subjected to a sudden step change in the base temperature. Few years later, Donaldson and Shouman [51] presented a study on the transient temperature distribution in a straight fin for a step change in base temperature and a step change in base heat flow rate. Also, in a subsequent works, Suryanarayana [52,53] investigated the transient response of straight fins of constant cross-sectional area. Mao and Rooke [54] utilized Laplace transform method to analyze straight fins for different cases of a step change in base temperature, a step change in base heat flux and a step change in fluid temperature. Method of Green's functions was adopted by Beck et al. [55] to study transient behavior of fins of constant cross-section area. In an earlier work, Kim [56] developed an approximate solution to the transient heat transfer in straight fins of constant cross-sectional area and constant physical and thermal properties. Three years later, Aziz and Na [57] examined the transient response of a semi-infinite fin of uniform thickness, initially at the ambient temperature, subjected to a step change in temperature at its base, with fin cooling governed by a power-law type dependence on temperature difference. In another work, Aziz and Kraus [58] presented a variety of analytical results for transient fins, developed by separation of variable and Laplace transform techniques. Campo and Salazar [59] explored the analogy between the transient conduction in a planar slab for short times and the steady state conduction in a straight fin of uniform cross-section. Saha and Acharya [60] submitted a detailed parametric analysis of the unsteady three-dimensional flow and heat transfer in a pin-fin heat exchanger. Furthermore, several numerical studies of transient fins combined with complicating factors, such as natural convection [61, 62], spatial arrays of fins [63, 64] and phase change materials [65] have been presented. Mutlu and Al-Shemmeri [66] studied a longitudinal array of straight fins suddenly heated at the base.

In the above reviewed studies, heat dissipation from the fin tip has been assumed negligible. Therefore, the analyses of the reviewed works were based on fins with insulated tips or negligible heat transfer at the tips. However, effects of fin tip on the thermal response and performance of the fin have been pointed out in some few studies in literature. In such studies, Irey [67], Laor and Kalman [68], Lau and Tau [69] and Ùnal [70] examined fins that dissipate heat also by their tips with constant or various temperature-dependence heat coefficients under steady state conditions.

Sequel to the above, there have been various studies on the thermal analysis of fin. However, there are limited studies in literatures on the applications of finite element methods for transient heat transfer analysis of fin with convective tip and under the influence of magnetic field. Therefore, in this present study, Galerkin finite element method is used study the transient thermal behavior of convective-radiative fin with convective tip and under the influence of magnetic field. The inherent advantages, wide range of applications and high level of accuracy of the method justify the consideration of the method for the problem under consideration. FEM is geometrically flexible and it enjoys an advantage in memory use and speed for large problems. It can handle Neumann boundary condition as readily as the Dirichlet boundary condition as demonstrated in the present study. Of all the numerical methods developed so far, the finite-element method has been found to be the most general method, not only to solve the problems of heat transfer but also to solve various problems in different areas of engineering and science. Finite element method provides superior versatility to other numerical methods and is generally very stable with excellent convergence characteristics. To the best of the authors' knowledge, the transient analysis of heat transfers in convective-radiative cooling fin with convective tip and subjected to magnetic field using finite element method has not been studied in open literature. As part of the aims of the present paper, a step-by-step finite element analysis is presented in this work. The numerical solutions are used to investigate the effects of convective, radiative, magnetic and convective tip parameters on the transient thermal performance of the cooling fin. Also, effect the thermal stability values for the various multi-boiling heat transfer modes are established.

2. Problem formulation

Consider a straight fin of length L and thickness t which is exposed on both faces to a convective-radiative environment at temperature T_∞ and subjected to a uniform magnetic field as shown in Fig.1. In order to develop the mathematical model governing the thermal behavior, the following assumptions are made:

I. The fin material is homogeneous and isotropic and with constant physical properties.
II. The thermal properties of the fin, surrounding medium and the magnetic field vary with temperature according to power-law. The temperature of the surrounding fluid is uniform.
III. The heat flow to or from the fin surface at any point is directly proportional to the temperature difference between the surface at that point and the surrounding fluid.
IV. The fin thickness is so small compared to its height and length that temperature gradients normal to the surface (across the fin thickness) may be neglected. Therefore, the temperature variation inside the fin is one-dimensional i.e. temperature varies along the fin length only. heat loss through the fin edges is negligible compared to that which passes through the sides.
V. There is no contact resistance where the base of the fin joins the prime surface. Also, the temperature of the base of the fin is uniform

VI. There are no heat sources or internal heat generation within the fin.

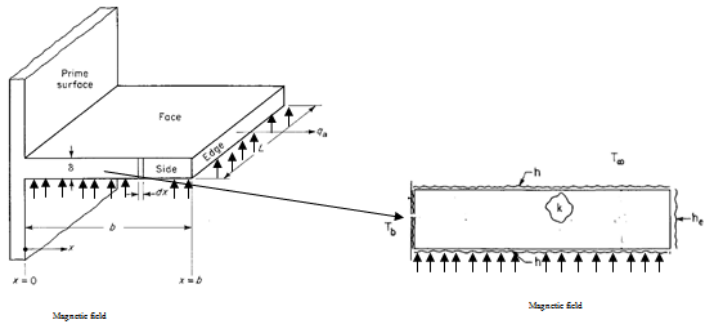

Fig. 1 (a) Schematic of longitudinal fin subjected to magnetic field(b) Computational domain of the fin

Based on following the above assumptions, the thermal energy balance could be expressed

$$q_x - \left(q_x + \frac{\delta q}{\delta x}dx\right) = h(T)P(T - T_\infty)dx + \sigma\varepsilon(T)P(T^4 - T_\infty^4)dx + \frac{\boldsymbol{J_c \times J_c}}{\sigma}dx + \rho A_{cr}c_p\frac{\partial T}{\partial t}dx \quad (1)$$

Where;

$$\mathrm{J_c} = \sigma(\mathrm{E} + \mathrm{V} \times \mathrm{B}) \quad (2)$$

As $dx \to 0$, Eq. (1) reduces

$$-\frac{dq}{dx} = h(T)P(T - T_a) + \sigma\varepsilon(T)P(T^4 - T_a^4) + \frac{\boldsymbol{J_c \times J_c}}{\sigma} + \rho A_{cr}c_p\frac{\partial T}{\partial t} \quad (3)$$

From Fourier's law of heat conduction, the rate of heat conduction in the fin is given by

$$\boldsymbol{q = -kA_{cr}\frac{dT}{dx}} \quad (4)$$

Following, the radiation heat transfer rate is

$$\boldsymbol{q = -kA_{cr}\frac{dT}{dx}} \quad (4)$$

$$q = -\frac{4\sigma A_{cr}}{3\beta_R}\frac{dT^4}{dx} \quad (5)$$

Therefore, the total rate of heat transfer is given by;

$$q = -kA_{cr}\frac{dT}{dx} - \frac{4\sigma A_{cr}}{3\beta_R}\frac{dT^4}{dx} \quad (6)$$

On substituting Eq. (6) into Eq. (3), one gets

$$\frac{d}{dx}\left(kA_{cr}\frac{dT}{dx}+\frac{4\sigma A_{cr}}{3\beta_R}\frac{dT^4}{dx}\right)=h(T)P(T-T_\infty)+\sigma(T)\varepsilon P(T^4-T_\infty^4)+\frac{\boldsymbol{J_c}\times\boldsymbol{J_c}}{\sigma}+\rho A_{cr}c_p\frac{\partial T}{\partial t} \tag{7}$$

Further simplification of Eq. (7) gives the governing differential equation for the fin as

$$\frac{d^2T}{dx^2}+\frac{4\sigma}{3\beta_R k}\frac{d}{dx}\left(\frac{dT^4}{dx}\right)-\frac{h(T)P}{kA_{cr}}(T-T_\infty)-\frac{\sigma\varepsilon(T)P}{kA_{cr}}(T^4-T_\infty^4)-\frac{\boldsymbol{J_c}\times\boldsymbol{J_c}}{\sigma kA_{cr}}=\frac{\rho c_p}{k}\frac{\partial T}{\partial t}, \tag{8}$$

The initial and boundary conditions are

$$\begin{aligned} &t=0, \quad 0<x<b, \quad T=T_b,\\ &t>0, \quad x=0, \quad T=T_b,\\ &t>0, \quad x=b, \quad -k\frac{dT}{dx}=h(T-T_\infty) \end{aligned} \tag{9a}$$

However, if the tip of the fin is assumed insulated or a negligible rate of heat transfer from it, we have

$$t>0, \quad x=b, \quad \frac{dT}{dx}=0 \tag{9b}$$

It should be noted that

$$\frac{\boldsymbol{J_c}\times\boldsymbol{J_c}}{\sigma}=\sigma_m B_o^2 u^2 \tag{10}$$

After substitution of Eq. (10) into Eq. (8),

$$\frac{d^2T}{dx^2}+\frac{4\sigma}{3\beta_R k}\frac{d}{dx}\left(\frac{dT^4}{dx}\right)-\frac{h(T)P}{kA_{cr}}(T-T_\infty)-\frac{\sigma\varepsilon(T)P}{kA_{cr}}(T^4-T_\infty^4)-\frac{\sigma_m(T)B_o^2u^2}{kA_{cr}}(T-T_\infty)=\frac{\rho c_p}{k}\frac{\partial T}{\partial t} \tag{11}$$

The first case that is considered in this work is a situation where small temperature difference exists within the fin material during the heat flow. This actually necessitated the use of temperature-invariant physical and thermal properties of the fin. Also, it has been established that under such scenario, the term T^4can be expressed as a linear function of temperature. Therefore, we have

$$T^4=T_\infty^4+4T_\infty^3(T-T_\infty)+6T_\infty^2(T-T_\infty)^2+\ldots\cong 4T_\infty^3T-3T_\infty^4 \tag{12}$$

Also, using Rosseland's approximation

$$\frac{4\sigma}{3\beta_R k}\frac{\partial T^4}{\partial x}\cong\frac{16\sigma T_\infty^3}{3\beta_R k}\frac{\partial^2 T}{\partial x^2} \tag{13}$$

On substituting Eqs. (15) and (16) into Eq. (14), we arrived at

$$\frac{d^2T}{dx^2}+\frac{16\sigma}{3\beta_R k}\frac{d^2T}{dx^2}-\frac{h(T)P}{kA_{cr}}(T-T_\infty)-\frac{4\sigma P\varepsilon(T)T_\infty^3}{kA_{cr}}(T-T_\infty)-\frac{\sigma_m(T)B_o^2u^2}{kA_{cr}}(T-T_\infty)=\frac{\rho c_p}{k}\frac{\partial T}{\partial t} \tag{14}$$

However, for most industrial applications the heat transfer coefficient may be given as the power law [2,19], where the exponent p and h_o are constants. The constant p may vary

between −6.6 and 5. However, in most practical applications it lies between −3 and 3 [19]. So, the power temperature-dependent thermal properties of the surrounding fluid and the magnetic field are defined as

$$h(T) = h_o\left(\frac{T - T_\infty}{T_b - T_\infty}\right)^p \tag{15}$$

Extending the same power temperature-dependent relationship to the fin emissivity and the magnetic field, we have

$$\varepsilon(T) = \varepsilon_o\left(\frac{T - T_\infty}{T_b - T_\infty}\right)^q \tag{16}$$

$$\sigma_m(T) = (\sigma_m)_o\left(\frac{T - T_\infty}{T_b - T_\infty}\right)^r \tag{17}$$

The exponent p on the heat transfer coefficient represents laminar film boiling or condensation when $p = -1/4$, laminar natural convection when $p = 1/4$, turbulent natural convection when $p = 1/3$, nucleate boiling when $p = 2$, radiation when $p = 3$. $p = 0$ implies a constant heat transfer coefficient.

Substitution of Eq. (16) - (17) gives

$$\frac{d^2T}{dx^2} + \frac{16\sigma}{3\beta_R k}\frac{d^2T}{dx^2} - \frac{h_o P(T - T_\infty)^{p+1}}{kA_{cr}(T_b - T_\infty)^p} - \frac{4\sigma\varepsilon_o P T_\infty^3 (T - T_\infty)^{q+1}}{kA_{cr}(T_b - T_\infty)^q} - \frac{\sigma_{m,o}B_o^2u^2(T - T_\infty)^{r+1}}{kA_{cr}(T_b - T_\infty)^r} = \frac{\rho c_p}{k}\frac{\partial T}{\partial t} \tag{18}$$

For constant thermal properties of the surrounding fluid and the magnetic field, we have a linear equation of the form

$$\frac{d^2T}{dx^2} + \frac{16\sigma}{3\beta_R k}\frac{d^2T}{dx^2} - \frac{hP(T - T_\infty)}{kA_{cr}} - \frac{4\sigma\varepsilon P T_\infty^3 (T - T_\infty)}{kA_{cr}} - \frac{\sigma_m B_o^2u^2(T - T_\infty)}{kA_{cr}} = \frac{\rho c_p}{k}\frac{\partial T}{\partial t} \tag{19}$$

It should be noted that the above Eq. (19) can be solved analytically. Using Laplace transform, it can easily be shown that the exact analytical solution of the equation based on the boundary conditions in Eq. (9) is given as;

$$T = T_\infty + (T_b - T_\infty)\left\{\frac{\left(\frac{(hP+4\sigma\varepsilon T_\infty^3 P+\sigma_m B_o^2u^2)L}{A_{cr}\left(k+\frac{16\sigma}{3\beta_R}\right)}\right)\cosh\left(\frac{(hP+4\sigma\varepsilon T_\infty^3 P+\sigma_m B_o^2u^2)}{A_{cr}\left(k+\frac{16\sigma}{3\beta_R}\right)}\right)(L-x)+\left(\frac{hL}{k}\right)\sinh\left(\frac{(hP+4\sigma\varepsilon T_\infty^3 P+\sigma_m B_o^2u^2)}{A_{cr}\left(k+\frac{16\sigma}{3\beta_R}\right)}\right)(L-x)}{\left(\frac{(hP+4\sigma\varepsilon T_\infty^3 P+\sigma_m B_o^2u^2)L}{A_{cr}\left(k+\frac{16\sigma}{3\beta_R}\right)}\right)\cosh\left(\frac{(hP+4\sigma\varepsilon T_\infty^3 P+\sigma_m B_o^2u^2)L}{A_{cr}\left(k+\frac{16\sigma}{3\beta_R}\right)}\right)+\left(\frac{hL}{k}\right)\sinh\left(\left(\frac{(hP+4\sigma\varepsilon T_\infty^3 P+\sigma_m B_o^2u^2)L}{A_{cr}\left(k+\frac{16\sigma}{3\beta_R}\right)}\right)\right)}\right.$$
$$\left. -2\sum_{n=1}^{\infty}\left\{\frac{\lambda_n^3\sin\left(\frac{\lambda_n x}{L}\right)\left\{exp-\left[\left(\lambda_n^2+\left(\frac{(hP+4\sigma\varepsilon T_\infty^3 P+\sigma_m B_o^2u^2)L}{A_{cr}\left(k+\frac{16\sigma}{3\beta_R}\right)}\right)^2\right)\left(\frac{\left(k+\frac{16\sigma}{3\beta_R}\right)t}{\rho c_p L^2}\right)\right]\right\}}{\left(\lambda_n^2+\left(\frac{(hP+4\sigma\varepsilon T_\infty^3 P+\sigma_m B_o^2u^2)L}{A_{cr}\left(k+\frac{16\sigma}{3\beta_R}\right)}\right)^2\right)\left(\left(\frac{hL}{k}\right)^2+\left(\frac{(hP+4\sigma\varepsilon T_\infty^3 P+\sigma_m B_o^2u^2)L}{A_{cr}\left(k+\frac{16\sigma}{3\beta_R}\right)}\right)^2+\frac{hL}{k}\right)\sin^2\lambda_n}\right\}\right. \tag{20a}$$

For the insulated tip, we have

$$T = T_\infty + (T_b - T_\infty)\left\{\begin{array}{l} \dfrac{\left(\frac{(hP+4\sigma\varepsilon T_\infty^3 P+\sigma_m B_0^2 u^2)L}{A_{cr}\left(k+\frac{16\sigma}{3\beta_R}\right)}\right)cosh\left(\frac{(hP+4\sigma\varepsilon T_\infty^3 P+\sigma_m B_0^2 u^2)}{A_{cr}\left(k+\frac{16\sigma}{3\beta_R}\right)}(L-x)\right)}{\left(\frac{(hP+4\sigma\varepsilon T_\infty^3 P+\sigma_m B_0^2 u^2)L}{A_{cr}\left(k+\frac{16\sigma}{3\beta_R}\right)}\right)cosh\left(\frac{(hP+4\sigma\varepsilon T_\infty^3 P+\sigma_m B_0^2 u^2)L}{A_{cr}\left(k+\frac{16\sigma}{3\beta_R}\right)}\right)} \\ -2\sum_{n=1}^{\infty}\left\{\dfrac{\lambda_n^3 sin\left(\frac{\lambda_n x}{L}\right)\left\{exp-\left[\left(\lambda_n^2+\left(\frac{(hP+4\sigma\varepsilon T_\infty^3 P+\sigma_m B_0^2 u^2)L}{A_{cr}\left(k+\frac{16\sigma}{3\beta_R}\right)}\right)^2\right)\left(\frac{\left(k+\frac{16\sigma}{3\beta_R}\right)t}{\rho c_p L^2}\right)\right]\right\}}{\left(\lambda_n^2+\left(\frac{(hP+4\sigma\varepsilon T_\infty^3 P+\sigma_m B_0^2 u^2)L}{A_{cr}\left(k+\frac{16\sigma}{3\beta_R}\right)}\right)^2\right)\left(\left(\frac{(hP+4\sigma\varepsilon T_\infty^3 P+\sigma_m B_0^2 u^2)L}{A_{cr}\left(k+\frac{16\sigma}{3\beta_R}\right)}\right)^2\right)sin^2\lambda_n}\right\} \end{array}\right\} \quad (20b)$$

where λ_n are the positive roots of the characteristic's equation

$$\lambda_n cos\lambda_n + \left(\frac{hL}{k}\right) sin\lambda_n = 0 \quad (21a)$$

It should be noted that a steady state is attained when $t \to \infty$

For the sake of convenience in subsequent analysis, it should be noted that "b" has been replaced with "L" in the above analytical solution.

3. Finite Element Method for the Transient Analysis

It is very difficult to develop exact analytical solution to the nonlinear equation in Eq. (14) or Eq. (18). Therefore, Galerkin finite element method is used in this work to solve the nonlinear equation. The procedures of the numerical method are outlined as follows:

I. **Finite element discretization**: The whole domain is divided into a finite number of sub-domains, designated as the discretization of the domain. Each sub-domain is called an element. The collection of elements comprises the finite-element mesh.

II. **Generation of the element equations**: From the mesh, a typical element is isolated and the variational formulation of the given problem over the typical element is constructed. An approximate solution of the variational problem is assumed and the element equations are generated by substituting the assumed solution in the formulation. The element matrix, which is called stiffness matrix, is constructed by using the element interpolation functions.

III. **Assembly of element equations**: The algebraic equations obtained from the element matrix are assembled by imposing the inter-element continuity conditions. This yields a large number of algebraic equations known as the global finite element model, which governs the whole domain.

IV. **Imposition of boundary conditions**: The essential and natural boundary conditions as given in the problem under consideration are imposed on the assembled equations.

V. **Solution of assembled equation**: The assembled equations after the imposition of the boundary conditions are solved by any numerical technique that is developed for solving systems of linear equations. The numerical techniques are

Gaussian elimination method, Gauss-Jordan iterative method, Gauss-Jacobi iterative method, Gauss-Seidel iterative method, LU decomposition method, Choleski decomposition, Crout's method, Householder's technique, etc.

In order to demonstrate the application of the finite element method to the present nonlinear problem, a weak formulation of the nonlinear governing differential equation is derived using Galerkin finite element method. For the purpose of the finite element analysis, one can rewrite Eq. (14) as;

$$\left(k+\frac{16\sigma}{3\beta_R}\right)\frac{d^2T}{dx^2}-\left(\frac{(h(T)P+4\sigma(T)P\varepsilon_o T_\infty^3+\sigma_m(T)B_o^2u^2)}{A_{cr}}\right)(T-T_\infty) \\ -\rho c_p\frac{\partial T}{\partial t}=0 \tag{21b}$$

where temperature-dependent thermal properties of the surrounding fluid and the magnetic field are defined in Eqs. (15) – (17). Using the shape/interpolating function on the governing equation and Integrating over the domain V of the control volume according to Galerkin finite element method, we have

$$\int_V W\left(\begin{array}{c}\left(k+\frac{16\sigma}{3\beta_R}\right)\frac{d^2T}{dx^2}-\left(\frac{(h(T)P+4\sigma(T)P\varepsilon_o T_\infty^3+\sigma_m(T)B_o^2u^2)}{A_{cr}}\right)(T-T_\infty)\\ -\rho c_p\frac{\partial T}{\partial t}=0\end{array}\right)dV=0 \tag{22}$$

For the one-dimensional problem which the dependent variable varies only along x-axis and the boundary integrals turn to be a point value on the boundaries, one can replace, dV by $A_{cr}dx$ in the Eq. (22). Here, A_{cr} is the uniform cross-sectional area of the fin and P is the perimeter of the fin from which convection takes place.

$$\int_L W\left(\begin{array}{c}\left(k+\frac{16\sigma}{3\beta_R}\right)\frac{d^2T}{dx^2}-\left(\frac{(h(T)P+4\sigma(T)P\varepsilon_o T_\infty^3+\sigma_m(T)B_o^2u^2)}{A_{cr}}\right)(T-T_\infty)\\ -\rho c_p\frac{\partial T}{\partial t}=0\end{array}\right)A_{cr}dx=0 \tag{23}$$

After expansion, one arrives at

$$\int_L W\left(\left(k+\frac{16\sigma}{3\beta_R}\right)\frac{\partial^2T}{\partial x^2}A_{cr}dx\right)-\int_L\left((h(T)P+4\sigma(T)\varepsilon_o T_\infty^3)P\right)(T-T_\infty)\,dx \\ -\int_L\sigma_m(T)B_o^2u^2(T-T_\infty)dx-\int_L\rho c\frac{\partial T}{\partial t}A_{cr}dx=0 \tag{24}$$

For the fin of length, L

$$\int_0^L W\left(\begin{array}{c}\left(k+\frac{16\sigma}{3\beta_R}\right)A_{cr}\frac{\partial^2T}{\partial x^2}-\left((h(T)P+4\sigma(T)\varepsilon_o T_\infty^3)P\right)(T-T_\infty)\\ -\sigma_m(T)B_o^2u^2(T-T_\infty)-\rho cA_{cr}\frac{\partial T}{\partial t}\end{array}\right)dx=0 \tag{25}$$

The expansion of Eq. (24) gives

$$\underbrace{\int_0^L W\left(k+\frac{16\sigma}{3\beta_R}\right)A_{cr}\frac{\partial}{\partial x}\left[\frac{\partial T}{\partial x}\right]dx}_{(1)}-\underbrace{\left[\begin{array}{c}\int_0^L(h(T)+4\sigma(T)\varepsilon_o T_\infty^3)PWT\,dx+\int_0^L\sigma_m(T)B_o^2u^2WT\,dx\\ -\int_0^L(h(T)+4\sigma(T)\varepsilon_o T_\infty^3)PT_\infty W\,dx-\int_0^L\sigma_m(T)B_o^2u^2WT_\infty dx\end{array}\right]}_{2}- \\ \underbrace{\int_0^L\rho c_pA_{cr}W\frac{\partial T}{\partial t}dx}_{3}=0 \tag{26}$$

For the term (1) in Eq. (26), one can write

$$\int_0^L W\left(k+\frac{16\sigma}{3\beta_R}\right)A_{cr}\frac{\partial}{\partial x}\left(\frac{\partial T}{\partial x}\right)dx=\left(k+\frac{16\sigma}{3\beta_R}\right)A_{cr}\int_0^L W\partial\left(\frac{\partial T}{\partial x}\right) \tag{27}$$

Applying integration by part$\left(\int_0^L u\partial v=uv|_0^L-\int_0^L v\,du\right)$ to Eq. (27), where;

$$=W\Rightarrow\frac{\partial u}{\partial x}=\frac{\partial W}{\partial x}and\partial v=\partial\left(\frac{\partial T}{\partial x}\right)\Rightarrow v=\frac{\partial T}{\partial x}u \tag{28}$$

Applying Eq. (28) in Eq. (27), gives

$$\begin{aligned}&\int_0^L\left(k+\frac{16\sigma}{3\beta_R}\right)A_{cr}W\frac{\partial}{\partial x}\left(\frac{\partial T}{\partial x}\right)dx=\left(k+\frac{16\sigma}{3\beta_R}\right)A_{cr}\int_0^L W\partial\left(\frac{\partial T}{\partial x}\right)\\&=\left(k+\frac{16\sigma}{3\beta_R}\right)A_{cr}\left\{W\frac{\partial T}{\partial x}\Big|_0^L-\int_0^L\frac{\partial W}{\partial x}\frac{\partial T}{\partial x}dx\right\}\end{aligned} \tag{29}$$

Substituting Eq. (29) into Eq. (26), leads to

$$\begin{aligned}&A_{cr}\left(k+\frac{16\sigma}{3\beta_R}\right)\frac{\partial T}{\partial x}\Big|_0^L W-\int_0^L\left(k+\frac{16\sigma}{3\beta_R}\right)A_{cr}\frac{\partial W}{\partial x}\frac{\partial T}{\partial x}dx\\&-\left[\begin{matrix}\int_0^L(h(T)+4\sigma(T)\varepsilon_oT_\infty^3)PWT\,dx+\int_0^L\sigma_m(T)B_o^2u^2WT\,dx\\-\int_0^L(h(T)+4\sigma(T)\varepsilon_oT_\infty^3)PT_\infty W\,dx-\int_0^L\sigma_m(T)B_o^2u^2WT_\infty d\,x\end{matrix}\right]-\int_0^L\rho c_pA_{cr}W\frac{\partial T}{\partial t}dx=0\end{aligned} \tag{30}$$

Eq. (30) can be written as

$$\begin{aligned}&\int_0^L\rho c_pA_{cr}W\frac{\partial T}{\partial t}dx+\int_0^L\left(k+\frac{16\sigma}{3\beta_R}\right)A_{cr}\frac{\partial W}{\partial x}\frac{\partial T}{\partial x}dx+\int_0^L(h(T)+4\sigma(T)\varepsilon_oT_\infty^3)PWT\,dx\\&\qquad+\int_0^L\sigma_m(T)B_o^2u^2WT\,dx\\&=\int_0^L(h(T)+4\sigma(T)\varepsilon_oT_\infty^3)PT_\infty W\,dx+\int_0^L\sigma_m(T)B_o^2u^2WT_\infty d\,x+A_{cr}\left(k+\frac{16\sigma}{3\beta_R}\right)\frac{\partial T}{\partial x}\Big|_0^L W\end{aligned} \tag{31}$$

The above Eq. (31) is a weak formulation of the nonlinear governing differential equation.

In order to carry out the finite element discretization as stated in the step 1 of the finite element analysis, the whole domain is divided into a finite number of sub-domains as shown in Fig. 2. For a one-dimensional problem, linear elements are used. The finite element discretization is done in a way such that the given length of the body is divided into number of divisions, say '*n*' elements which consequently, gives *(n + 1)* nodes to represent the body as shown in Table 1.

Table 1. Element and node numbers of linearone-dimensional elements

Element No.	Node *i*	Node *j*
1	*1*	*2*
2	*2*	*3*
3	*3*	*4*
e	*i*	*j*
n	*n*	*n+1*

Table 2. Element and node numbers of linear one-dimensionalelements used in this study

Element No.	Node *i*	Node *j*
1	*1*	*2*
2	*2*	*3*
3	*3*	*4*
.	.	.
.	.	.
.	.	.
48	*48*	*49*
49	*49*	*50*
50	*50*	*51*

In the finite element analysis of the present problem (one-dimension transient state), 2-node linear elements are used and the given length of the fin is divided into 50 elements which give 51 nodes to represent the total length of the fin as shown in Table 2 and Fig. 2.

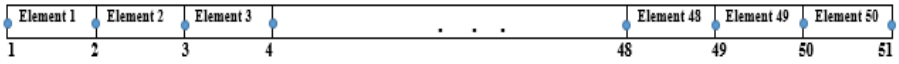

Fig. 2. Finite element

In order to construct a variational formulation of the given problem over an element, a typical element is isolated (Fig. 3) from the mesh shown in Fig. 2. The typical 2-node linear element with end nodes '*i*' and '*j*' having the corresponding temperature being denoted by T_i and T_j, respectively is shown in Fig. 3.

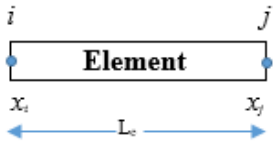

Fig. 3. A 2-node element

For the 2-node element, the following analysis for the variational formulation is carried out. Following Eq. (31), it could be stated that the weak form formulation of the governing Equation for an element of length "L_e" is given as

$$\int_0^{L_e} \rho c_p A_{cr} W \frac{\partial T}{\partial t} dx + \int_0^{L_e} \left(k + \frac{16\sigma}{3\beta_R}\right) A_{cr} \frac{\partial W}{\partial x} \frac{\partial T}{\partial x} dx + \int_0^{L_e} (h(T) + 4\sigma(T)\varepsilon_o T_\infty^3) PWT\, dx + \int_0^{L_e} \sigma_m(T) B_o^2 u^2 WT\, dx = \int_0^{L_e} (h(T) + 4\sigma(T)\varepsilon_o T_\infty^3) PT_\infty W\, dx + \int_0^{L_e} \sigma_m(T) B_o^2 u^2 WT_\infty d\, x + A_{cr} \left(k + \frac{16\sigma}{3\beta_R}\right) \frac{\partial T}{\partial x}\Big|_0^{L_e} W \tag{32}$$

The linear temperature variation in the element is represented by

$$T = \lambda_1 + \lambda_2 x \tag{33}$$

where T is the temperature at any location x and the parameters λ_1 and λ_2 are constants. Since there are two arbitrary constants in the linear representation, it requires only two nodes to determine the values of λ_1 and λ_2. Thus, we have

$$T_i = \lambda_1 + \lambda_2 x_i \tag{34a}$$

$$T_j = \lambda_1 + \lambda_2 x_j \tag{34b}$$

On solving Eq. (34a) and (34b), we have

$$\lambda_1 = \frac{T_i x_j - T_j x_i}{x_j - x_i}, \qquad \lambda_2 = \frac{T_j - T_i}{x_j - x_i} \tag{35}$$

After substituting the values of λ_1 and λ_2 in Eq. (35) into Equ. (33), one arrives at

$$T = T_i\left(\frac{x_j - x}{x_j - x_i}\right) + T_j\left(\frac{x - x_i}{x_j - x_i}\right) \tag{36}$$

The above Eq. (36) can be written as

$$T = T_i W_i + T_j W_j = \begin{bmatrix} W_i & W_j \end{bmatrix}\begin{Bmatrix} T_i \\ T_j \end{Bmatrix} \tag{37}$$

Where

$$W_i = \frac{x_j - x}{x_j - x_i}, \qquad W_j = \frac{x - x_i}{x_j - x_i} \tag{38}$$

W_i and W_j are called shape/interpolation/test/basis functions. Furthermore, one can write Equ. (37) as;

$$T = [\boldsymbol{W}]\{\boldsymbol{T}\} \tag{39}$$

Where;

$$[\boldsymbol{W}] = \begin{bmatrix} W_i & W_j \end{bmatrix} \tag{40}$$

is the shape function matrix and

$$\{\boldsymbol{T}\} = \begin{bmatrix} T_i \\ T_j \end{bmatrix} \tag{41}$$

is the vector of unknown temperatures taking

$$x_i = 0, \quad x_j = L_e, \quad \Rightarrow x_j - x_i = L_e \tag{42}$$

Substitute Eq. (42) into Eq. (38), we have the shape functions as;

$$W_i = 1 - \frac{x}{L_e}, W_j = \frac{x}{L_e} \tag{43}$$

On substituting Eq. (43) into Eq. (37), we can see that the temperature at any point "x" in the 2-node element is approximated by;

$$T = \left(1 - \frac{x}{L_e}\right)T_i + \left(\frac{x}{L_e}\right)T_j \quad \Rightarrow T = T_i W_i + T_j W_j T = \begin{bmatrix} W_i & W_j \end{bmatrix}\begin{Bmatrix} T_i \\ T_j \end{Bmatrix} = [\boldsymbol{W}]\{\boldsymbol{T}\} \tag{44}$$

Therefore

$$\frac{\partial T}{\partial t}=\left(1-\frac{x}{L_e}\right)\frac{\partial T_i}{\partial t}+\left(\frac{x}{L_e}\right)\frac{\partial T_j}{\partial t}\quad\Rightarrow\frac{\partial T}{\partial t}=W_i\frac{\partial T_i}{\partial t}+W_j\frac{\partial T_j}{\partial t}=\begin{bmatrix}W_i & W_j\end{bmatrix}\begin{Bmatrix}\frac{\partial T_i}{\partial t}\\ \frac{\partial T_j}{\partial t}\end{Bmatrix}=[\boldsymbol{W}]\left\{\frac{\partial \boldsymbol{T}}{\partial t}\right\} \tag{45}$$

$$\frac{\partial T}{\partial x}=\frac{\partial T}{\partial x}=\frac{\partial W_i}{\partial x}T_i+\frac{\partial W_j}{\partial x}T_j=\left(-\frac{1}{L_e}\right)T_i+\left(\frac{1}{L_e}\right)T_j=\frac{1}{L_e}(T_j-T_i)\quad\Rightarrow T=\begin{bmatrix}-\frac{1}{L_e} & \frac{1}{L_e}\end{bmatrix}\begin{Bmatrix}T_i\\ T_j\end{Bmatrix} \tag{46}$$
$$=[\boldsymbol{B}]\{\boldsymbol{T}\}$$

Where;

$$[\boldsymbol{B}]=\begin{bmatrix}\frac{\partial W_i}{\partial x} & \frac{\partial W_j}{\partial x}\end{bmatrix} \tag{47}$$

After substitution of Eq. (44), (45), (46) and (47) into Eq. (32), we have

$$\begin{aligned}&\int_0^{L_e}\rho c_p A_{cr}\begin{bmatrix}W_i\\ W_j\end{bmatrix}\begin{bmatrix}W_i & W_j\end{bmatrix}\begin{Bmatrix}\frac{\partial T_i}{\partial t}\\ \frac{\partial T_j}{\partial t}\end{Bmatrix}dx+\int_0^{L_e}\left(k+\frac{16\sigma}{3\beta_R}\right)A_{cr}\begin{bmatrix}\frac{\partial W_i}{\partial x}\\ \frac{\partial W_j}{\partial x}\end{bmatrix}\begin{bmatrix}\frac{\partial W_i}{\partial x} & \frac{\partial W_j}{\partial x}\end{bmatrix}\begin{Bmatrix}T_i\\ T_j\end{Bmatrix}dx\\ &+\int_0^{L_e}(h(T)+4\sigma(T)\varepsilon_o T_\infty^3)P\begin{bmatrix}W_i\\ W_j\end{bmatrix}\begin{bmatrix}W_i & W_j\end{bmatrix}\begin{Bmatrix}T_i\\ T_j\end{Bmatrix}dx\\ &+\int_0^{L_e}\sigma_m(T)B_o^2u^2\begin{bmatrix}W_i\\ W_j\end{bmatrix}\begin{bmatrix}W_i & W_j\end{bmatrix}\begin{Bmatrix}T_i\\ T_j\end{Bmatrix}dx\\ &=\int_0^{L_e}(h(T)+4\sigma(T)\varepsilon_o T_\infty^3)PT_\infty\begin{bmatrix}W_i\\ W_j\end{bmatrix}dx+\int_0^{L_e}\sigma_m(T)B_o^2u^2T_\infty\begin{bmatrix}W_i\\ W_j\end{bmatrix}d\,x\\ &+A_{cr}\left(k+\frac{16\sigma}{3\beta_R}\right)\frac{\partial T}{\partial x}\Big|_0^{L_e}\begin{bmatrix}W_i\\ W_j\end{bmatrix}\end{aligned} \tag{48}$$

Eq. (48) can be written as

$$\begin{aligned}&\int_0^{L_e}\rho c_p A_{cr}\begin{bmatrix}W_i & W_j\end{bmatrix}^T\begin{bmatrix}W_i & W_j\end{bmatrix}\begin{Bmatrix}\frac{\partial T_i}{\partial t}\\ \frac{\partial T_j}{\partial t}\end{Bmatrix}dx\\ &+\int_0^{L_e}\left(k+\frac{16\sigma}{3\beta_R}\right)A_{cr}\begin{bmatrix}\frac{\partial W_i}{\partial x} & \frac{\partial W_j}{\partial x}\end{bmatrix}^T\begin{bmatrix}\frac{\partial W_i}{\partial x} & \frac{\partial W_j}{\partial x}\end{bmatrix}\begin{Bmatrix}T_i\\ T_j\end{Bmatrix}dx\\ &+\int_0^{L_e}(h(T)+4\sigma(T)\varepsilon_o T_\infty^3)P\begin{bmatrix}W_i & W_j\end{bmatrix}^T\begin{bmatrix}W_i & W_j\end{bmatrix}\begin{Bmatrix}T_i\\ T_j\end{Bmatrix}dx\\ &+\int_0^{L_e}\sigma_m(T)B_o^2u^2\begin{bmatrix}W_i & W_j\end{bmatrix}^T\begin{bmatrix}W_i & W_j\end{bmatrix}\begin{Bmatrix}T_i\\ T_j\end{Bmatrix}dx\\ &=\int_0^{L_e}(h(T)+4\sigma(T)\varepsilon_o T_\infty^3)PT_\infty\begin{bmatrix}W_i & W_j\end{bmatrix}^T dx+\int_0^{L_e}\sigma_m(T)B_o^2u^2T_\infty\begin{bmatrix}W_i & W_j\end{bmatrix}^T d\,x\\ &+A_{cr}\left(k+\frac{16\sigma}{3\beta_R}\right)\frac{\partial T}{\partial x}\Big|_0^{L_e}\begin{bmatrix}W_i & W_j\end{bmatrix}^T\end{aligned} \tag{49}$$

For the *i* and *j* nodes of an element, Eq. (49) can be written in a convenient form as

$$[C_{ij}]\begin{Bmatrix}\frac{\partial T_i}{\partial t}\\ \frac{\partial T_j}{\partial t}\end{Bmatrix}+[K_{ij}(T)]\begin{Bmatrix}T_i\\ T_j\end{Bmatrix}=[f_{ij}(T)] \tag{50}$$

Where

$$[C_{ij}]=\int_0^{L_e}\rho c_p A_{cr}\begin{bmatrix}W_i & W_j\end{bmatrix}^T\begin{bmatrix}W_i & W_j\end{bmatrix}dx \tag{51}$$

$$[K_{ij}(T)]=\int_0^{L_e}\left(k+\frac{16\sigma}{3\beta_R}\right)A_{cr}\begin{bmatrix}\frac{\partial W_i}{\partial x} & \frac{\partial W_j}{\partial x}\end{bmatrix}^T\begin{bmatrix}\frac{\partial W_i}{\partial x} & \frac{\partial W_j}{\partial x}\end{bmatrix}dx \tag{52}$$

$$+\int_0^{L_e}\sigma_m(T)B_o^2u^2\begin{bmatrix}W_i & W_j\end{bmatrix}^T\begin{bmatrix}W_i & W_j\end{bmatrix}dx$$
$$[f_{ij}(T)]=\int_0^{L_e}(h(T)+4\sigma(T)\varepsilon_oT_\infty^3)PT_\infty\begin{bmatrix}W_i & W_j\end{bmatrix}^T dx$$
$$+\int_0^{L_e}\sigma_m(T)B_o^2u^2T_\infty\begin{bmatrix}W_i & W_j\end{bmatrix}^T d\,x \tag{53}$$
$$+A_{cr}\left(k+\frac{16\sigma}{3\beta_R}\right)\frac{\partial T}{\partial x}\Big|_0^{L_e}\begin{bmatrix}W_i & W_j\end{bmatrix}^T,$$

Alternatively, using the relationships in Eqs. (44) - (46), one can write Eq. (49) in a compact matrix form of as;

$$\int_0^{L_e}\rho c_pA_{cr}[\boldsymbol{W}]^T[\boldsymbol{W}]\left\{\frac{\partial \boldsymbol{T}}{\partial t}\right\}dx+\int_0^{L_e}\left(k+\frac{16\sigma}{3\beta_R}\right)A_{cr}[\boldsymbol{B}]^T[\boldsymbol{B}][\boldsymbol{T}]\,dx$$
$$+\int_0^{L_e}(h(T)+4\sigma(T)\varepsilon_oT_\infty^3)P[\boldsymbol{W}]^T[\boldsymbol{W}][\boldsymbol{T}]\,dx+\int_0^{L_e}\sigma_m(T)B_o^2u^2[\boldsymbol{W}]^T[\boldsymbol{W}][\boldsymbol{T}]\,dx \tag{54}$$
$$=\int_0^{L_e}(h(T)+4\sigma(T)\varepsilon_oT_\infty^3)P[\boldsymbol{W}]^TT_\infty\,dx+\left(A_{cr}\left(k+\frac{16\sigma}{3\beta_R}\right)\frac{\partial T}{\partial x}\right)\Big|_0^{L_e}[\boldsymbol{W}]^T$$

Eq. (54) can be written form as;

$$[\boldsymbol{C}]\left\{\frac{\partial \boldsymbol{T}}{\partial t}\right\}+[\boldsymbol{K}(T)]\{\boldsymbol{T}\}=[\boldsymbol{f}(T)] \tag{55}$$

Where

$$[\boldsymbol{C}]=\int_0^{L_e}\rho c_pA[\boldsymbol{W}]^T[\boldsymbol{W}]dx \tag{56}$$

$$[\boldsymbol{K}(T)]=\int_0^{L_e}\left(k+\frac{16\sigma}{3\beta_R}\right)A_{cr}[\boldsymbol{B}]^T[\boldsymbol{B}]\,dx+\int_0^{L_e}(h(T)+4\sigma(T)\varepsilon_oT_\infty^3)P[\boldsymbol{W}]^T[\boldsymbol{W}]\,dx \tag{57}$$
$$+\int_0^{L_e}\sigma_m(T)B_o^2u^2[\boldsymbol{W}]^T[\boldsymbol{W}]\,dx$$

$$[\boldsymbol{f}(T)]=\int_0^{L_e}(h(T)+4\sigma(T)\varepsilon_oT_\infty^3)PT_\infty[\boldsymbol{W}]^TT_\infty\,dx+\int_0^{L_e}\sigma_m(T)B_o^2u^2T_\infty[\boldsymbol{W}]^TT_\infty\,dx \tag{58}$$
$$+A\left(\left(k+\frac{16\sigma}{3\beta_R}\right)\frac{\partial T}{\partial x}\right)\Big|_0^{L_e}[\boldsymbol{W}]^T$$

In order to develop the matrix equation for the element, we need to expand Eq. (51) - (54) or the equivalent equations in Eq. (56) – (58). Therefore, the expansions are carried out as follows

$$[C_{ij}]=\int_0^{L_e}\rho c_p\,A_{cr}\begin{bmatrix}W_i & W_j\end{bmatrix}^T\begin{bmatrix}W_i & W_j\end{bmatrix}dx=\int_0^{L_e}\rho c_pA_{cr}\begin{bmatrix}W_i^2 & W_iW_j\\ W_iW_j & W_j^2\end{bmatrix}dx, \tag{59}$$

$$[K_{ij}(T)]=\int_0^{L_e}\left(k+\frac{16\sigma}{3\beta_R}\right)A_{cr}\begin{bmatrix}\left(\frac{\partial W_i}{\partial x}\right)^2 & \frac{\partial W_i}{\partial x}\frac{\partial W_j}{\partial x}\\ \frac{\partial W_i}{\partial x}\frac{\partial W_j}{\partial x} & \left(\frac{\partial W_j}{\partial x}\right)^2\end{bmatrix}\begin{Bmatrix}T_i\\T_j\end{Bmatrix}dx$$
$$+\int_0^{L_e}(h(T)+4\sigma(T)\varepsilon_oT_\infty^3)P\begin{bmatrix}W_i^2 & W_iW_j\\ W_iW_j & W_j^2\end{bmatrix}\begin{Bmatrix}T_i\\T_j\end{Bmatrix}dx \tag{60}$$
$$+\int_0^{L_e}\sigma_m(T)B_o^2u^2\begin{bmatrix}W_i^2 & W_iW_j\\ W_iW_j & W_j^2\end{bmatrix}\begin{Bmatrix}T_i\\T_j\end{Bmatrix}dx$$

$$[f_{ij}(T)]=\int_0^{L_e}(h(T)+4\sigma(T)\varepsilon_oT_\infty^3)PT_\infty\begin{bmatrix}W_i\\W_j\end{bmatrix}dx \tag{61}$$

$$+\int_0^{L_e}\sigma_m(T)B_o^2u^2T_\infty\begin{bmatrix}W_i\\W_j\end{bmatrix}d\,x+A_{cr}\left(k+\frac{16\sigma}{3\beta_R}\right)\frac{\partial T}{\partial x}\Big|_0^{L_e}\begin{bmatrix}W_i\\W_j\end{bmatrix}$$

On substituting Eq. (43) into Eq. (46) into the above Eqs. (59) -(61), one arrives. For the global capacitance matrix, we have

$$[C_{ij}]=\int_0^{L_e}\rho c_p\begin{bmatrix}\left(1-\frac{x}{L_e}\right)^2 & \left(1-\frac{x}{L_e}\right)\left(\frac{x}{L_e}\right)\\ \left(1-\frac{x}{L_e}\right)\left(\frac{x}{L_e}\right) & \left(\frac{x}{L_e}\right)^2\end{bmatrix}dx \tag{62}$$

For the stiffness matrix;

$$\begin{aligned}[K_{ij}(T)]=&\int_0^{L_e}\left(k+\frac{16\sigma}{3\beta_R}\right)A_{cr}\begin{bmatrix}\left(-\frac{1}{L_e}\right)^2 & \left(-\frac{1}{L_e}\right)\left(\frac{1}{L_e}\right)\\ \left(-\frac{1}{L_e}\right)\left(\frac{1}{L_e}\right) & \left(\frac{1}{L_e}\right)^2\end{bmatrix}dx\\&+\int_0^{L_e}(h(T)+4\sigma(T)\varepsilon_oT_\infty^3)P\begin{bmatrix}\left(1-\frac{x}{L_e}\right)^2 & \left(1-\frac{x}{L_e}\right)\left(\frac{x}{L_e}\right)\\ \left(1-\frac{x}{L_e}\right)\left(\frac{x}{L_e}\right) & \left(\frac{x}{L_e}\right)^2\end{bmatrix}dx\\&+\int_0^{L_e}\sigma_m(T)B_o^2u^2\begin{bmatrix}\left(1-\frac{x}{L_e}\right)^2 & \left(1-\frac{x}{L_e}\right)\left(\frac{x}{L_e}\right)\\ \left(1-\frac{x}{L_e}\right)\left(\frac{x}{L_e}\right) & \left(\frac{x}{L_e}\right)^2\end{bmatrix}dx\end{aligned} \tag{63}$$

For the load vector

$$\begin{aligned}[f_i(T)]=&\int_0^{L_e}(h(T)+4\sigma(T)\varepsilon_oT_\infty^3)P\begin{bmatrix}\left(1-\frac{x}{L_e}\right)\\ \left(\frac{x}{L_e}\right)\end{bmatrix}T_\infty\,dx+\int_0^{L_e}\sigma_m(T)B_o^2u^2\begin{bmatrix}\left(1-\frac{x}{L_e}\right)\\ \left(\frac{x}{L_e}\right)\end{bmatrix}T_\infty\,dx\\&+A_{cr}\left(\left(k+\frac{16\sigma}{3\beta_R}\right)\frac{\partial T}{\partial x}\right)\Big|_0^{L_e}\begin{bmatrix}\left(1-\frac{x}{L_e}\right)\\ \left(\frac{x}{L_e}\right)\end{bmatrix}\end{aligned} \tag{64}$$

After the integrations, we have the global capacitance matrix, stiffness matrix and the load vector as;

$$[C_{ij}]=\frac{\rho c_pAL_e}{6}\begin{bmatrix}2&1\\1&2\end{bmatrix} \tag{65}$$

$$[K_{ij}(T)]=\left[\frac{\left(k+\frac{16\sigma}{3\beta_R}\right)A_{cr}}{L_e}\begin{bmatrix}1&-1\\-1&1\end{bmatrix}+\frac{(h(T)+4\sigma(T)\varepsilon_oT_\infty^3)PL_e}{6}\begin{bmatrix}2&1\\1&2\end{bmatrix}+\frac{\sigma_m(T)B_o^2u^2L_e}{6}\begin{bmatrix}2&1\\1&2\end{bmatrix}\right] \tag{66}$$

$$[f_i(T)]=\frac{(h(T)+4\sigma(T)\varepsilon_oT_\infty^3)PT_\infty L_e+\sigma_m(T)B_o^2u^2T_\infty L}{2}\begin{bmatrix}1\\1\end{bmatrix}+\left(k+\frac{16\sigma}{3\beta_R}\right)A_{cr}\begin{bmatrix}-\frac{\partial T(0)}{\partial x}\\ \frac{\partial T(L_e)}{\partial x}\end{bmatrix} \tag{67}$$

Substitution Eq. (65) – (67) into Eq. (50), gives the characteristic equation over the space interval Δx as;

$$\frac{\rho c_pAL_e}{6}\begin{bmatrix}2&1\\1&2\end{bmatrix}\begin{Bmatrix}\frac{\partial T_i}{\partial t}\\ \frac{\partial T_i}{\partial t}\end{Bmatrix}+\left[\frac{\left(k+\frac{16\sigma}{3\beta_R}\right)A_{cr}}{L}\begin{bmatrix}1&-1\\-1&1\end{bmatrix}+\frac{(h(T)+4\sigma(T)\varepsilon_oT_\infty^3)PL_e}{6}\begin{bmatrix}2&1\\1&2\end{bmatrix}\right. \tag{68}$$

$$== \frac{(h(T)+4\sigma(T)\varepsilon_o T_\infty^3)PT_\infty L_e}{2}\begin{bmatrix}1\\1\end{bmatrix}+\frac{\sigma_m(T)B_o^2u^2T_\infty L_e}{2}\begin{bmatrix}1\\1\end{bmatrix}+\left(k+\frac{16\sigma}{3\beta_R}\right)A_{cr}\begin{bmatrix}-\frac{\partial T(0)}{\partial x}\\ \frac{\partial T(L_e)}{\partial x}\end{bmatrix}$$

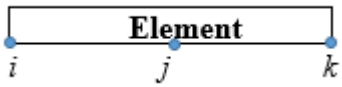

Fig. 4. A 3-node element

The steps above are general. Both the results and the analysis can be different if one uses 3-node element. Using a 3-node element, one arrives at

$$[C_{ij}]\begin{Bmatrix}\frac{\partial T_i}{\partial t}\\ \frac{\partial T_j}{\partial t}\\ \frac{\partial T_k}{\partial t}\end{Bmatrix}+[K_{ij}(T)]\begin{Bmatrix}T_i\\T_j\\T_k\end{Bmatrix}=[f_{ij}(T)] \tag{69}$$

Where;

$$[C_{ij}]=\frac{\rho c_p A_{cr}L_e}{6}\begin{bmatrix}8&4&-2\\4&32&4\\-2&4&8\end{bmatrix} \tag{70}$$

$$[K_{ij}(T)]=\left[\frac{\left(k+\frac{16\sigma}{3\beta_R}\right)A_{cr}}{3L_e}\begin{bmatrix}7&-8&1\\-8&16&-8\\1&-8&7\end{bmatrix}+(h(T)P+4\sigma(T)\varepsilon_o T_\infty^3 P+\sigma_m(T)B_o^2u^2)\frac{L_e}{60}\begin{bmatrix}8&4&-2\\4&32&4\\-2&4&8\end{bmatrix}\right] \tag{71}$$

$$[f_i(T)]=(h(T)P+4\sigma(T)\varepsilon_o T_\infty^3 P+\sigma_m(T)B_o^2u^2)\frac{T_\infty L_e}{6}\begin{bmatrix}1\\4\\1\end{bmatrix}+\left(k+\frac{16\sigma}{3\beta_R}\right)A_{cr}\begin{bmatrix}-\frac{\partial T(0)}{\partial x}\\ \frac{\partial T(M)}{\partial x}\\ \frac{\partial T(L)}{\partial x}\end{bmatrix} \tag{72}$$

After the substitution of Eqs. (69) - (72), we arrived at

$$\frac{\rho c_p A_{cr} L_e}{6}\begin{bmatrix}8 & 4 & -2\\ 4 & 32 & 4\\ -2 & 4 & 8\end{bmatrix}\begin{Bmatrix}\frac{\partial T_i}{\partial t}\\ \frac{\partial T_j}{\partial t}\\ \frac{\partial T_k}{\partial t}\end{Bmatrix} + \left[\frac{\left(k+\frac{16\sigma}{3\beta_R}\right)A_{cr}}{3L_e}\begin{bmatrix}7 & -8 & 1\\ -8 & 16 & -8\\ 1 & -8 & 7\end{bmatrix} + (h(T)P + 4\sigma(T)\varepsilon_o T_\infty^3 P + \sigma_m(T)B_o^2u^2)\frac{L_e}{60}\begin{bmatrix}8 & 4 & -2\\ 4 & 32 & 4\\ -2 & 4 & 8\end{bmatrix}\right]\begin{Bmatrix}T_i\\ T_j\\ T_k\end{Bmatrix}$$
$$= (h(T)P + 4\sigma(T)\varepsilon_o T_\infty^3 P + \sigma_m(T)B_o^2u^2)\frac{T_\infty L_e}{6}\begin{bmatrix}1\\ 4\\ 1\end{bmatrix} + \left(k+\frac{16\sigma}{3\beta_R}\right)A_{cr}\begin{bmatrix}-\frac{\partial T(0)}{\partial x}\\ \frac{\partial T(M)}{\partial x}\\ \frac{\partial T(L)}{\partial x}\end{bmatrix} \quad (73)$$

3.1. Time discretization using the Finite Difference Method (FDM)

The above equation is a general representation of a one-dimensional problem with one linear element. All the terms are included irrespective of the boundary condition. Eq. (50) or (55) is semi-discrete as it is discretized only in space. The differential operator still contains the time-dependent term and it has to be discretized. We now require a method of discretizing the transient terms of the equation. The following subsections give the details of how the transient terms is discretized.

$$[C_{ij}]\begin{Bmatrix}\frac{T_i^{m+1}-T_i^m}{\Delta t}\\ \frac{T_j^{m+1}-T_j^m}{\Delta t}\end{Bmatrix} + [K_{ij}(T)]\begin{Bmatrix}\theta T_i^{m+1}+(1-\theta)T_i^m\\ \theta T_j^{m+1}+(1-\theta)T_j^{m+1}\end{Bmatrix} = \begin{Bmatrix}\theta f_i^{m+1}+(1-\theta)f_i^m\\ \theta f_j^{m+1}+(1-\theta)f_j^{m+1}\end{Bmatrix} \quad (74)$$

which can be compactly written as;

$$[\boldsymbol{C}]\left\{\frac{\{\boldsymbol{T}^{m+1}-\boldsymbol{T}^m\}}{\Delta t}\right\} + [\boldsymbol{K}(T)]\{\theta\boldsymbol{T}^{m+1}+(1-\theta)\boldsymbol{T}^m\} = \{\theta\boldsymbol{f}^{m+1}+(1-\theta)\boldsymbol{f}^m\} \quad (75)$$

Therefore,

$$\left[[\boldsymbol{C}]+\theta\Delta t[\boldsymbol{K}(T)]\right]\boldsymbol{T}^{m+1} = \left[[\boldsymbol{C}]-(1-\theta)\Delta t[\boldsymbol{K}(T)]\right]\boldsymbol{T}^m + \Delta t\{\theta\boldsymbol{f}^{m+1}+(1-\theta)\boldsymbol{f}^m\} \quad (76)$$

where, "m" denotes the time level.

Table 3. Different time-stepping schemes

θ	Name of the Scheme	Comments
0.0	Fully explicit scheme	Forward different method
1.0	Fully implicit scheme	Backward difference method
0.5	Semi-implicit scheme	Crank-Nicolson method

Eq. (76) gives the nodal values of temperature at the $m + 1$, time level. These temperature values are calculated using the m time level values. However, both the $m + 1$ and m time level values of the forcing vector $\{\mathbf{f}\}$ must be known. By varying the parameter θ, different transient schemes can be constructed, which are shown in Table 4 for varying values of θ. Therefore, for the temporal discretization, two-level θ method has been used for the analysis. This approach varies between explicit and implicit strategies and results in the algebraic systems of nonlinear equations.

It is very difficult to provide explicit solutions to the developed systems of nonlinear equations. Therefore, recourse is made to use an iterative predictor-corrector scheme, based on direct substitution iteration to handle nonlinearity in the present analysis. Based on the name, this scheme is an algorithm that proceeds in two steps, namely; the predictor step and then the corrector step. It calculates a rough approximation of the desired quantity in the predictor step and refines the approximation in the corrector step. This scheme combines the advantages associated with explicit and implicit time schemes and hence provides the stable solution to solve complex nonlinear problems (Lewis and Roberts [51]). The steps are shown as follows:

Predictor

$$\begin{aligned}&\left[[\boldsymbol{C}(\boldsymbol{T}^m)]+\theta\Delta t\boldsymbol{A}(\boldsymbol{T}^m)\right]\boldsymbol{T}_*^{m+1}\\&=\left[[\boldsymbol{C}(\boldsymbol{T}^m)]-(1-\theta)\Delta t\boldsymbol{A}(\boldsymbol{T}^m)\right]\boldsymbol{T}^m+\Delta t\{\theta\boldsymbol{B}(\boldsymbol{T}^m)\boldsymbol{f}^{m+1}+\boldsymbol{B}(\boldsymbol{T}^m)(1-\theta)\boldsymbol{f}^m\}\end{aligned} \tag{77}$$

Corrector

$$\begin{aligned}&\left[\left[\boldsymbol{C}(\boldsymbol{T}_p^{\bar{m}})\right]+\theta\Delta t\boldsymbol{A}(\boldsymbol{T}_p^{\bar{m}})\right]\boldsymbol{T}_p^{m+1}\\&=\left[\left[\boldsymbol{C}(\boldsymbol{T}_p^{\bar{m}})\right]-(1-\theta)\Delta t\boldsymbol{A}(\boldsymbol{T}_p^{\bar{m}})\right]\boldsymbol{T}^m+\Delta t\{\theta\boldsymbol{B}(\boldsymbol{T}_p^{\bar{m}})\boldsymbol{f}^{m+1}+\boldsymbol{B}(\boldsymbol{T}_p^{\bar{m}})(1-\theta)\boldsymbol{f}^m\}\end{aligned} \tag{78}$$

Where p = 0,1,2, 3… up to convergence

$$\boldsymbol{T}_p^{\bar{m}}=w\boldsymbol{T}_p^{m+1}+(1-w)\boldsymbol{T}^m \quad 0\le w\le 1 \tag{79a}$$

$$\boldsymbol{T}_0^{m+1}=\boldsymbol{T}_*^{m+1} \tag{79b}$$

3.2. Time discretization using the Finite Element Method

Alternatively, the temporal term in the transient equation can be discretized by using finite element method to discretize Eq. (76) in the time domain. In Equ. (76), the temperature is now discretized in the time domain as in Fig. (4).

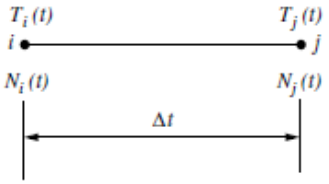

Fig. 5 Time discretization between nth (i) and n + 1th (j) time levels

$$T(t)=N_i(t)T_i(t)+N_j(t)T_j(t)=\begin{bmatrix}N_i(t) & N_j(t)\end{bmatrix}\begin{Bmatrix}T_i(t)\\T_j(t)\end{Bmatrix} \tag{80}$$

Following the similar procedure as done previously, we can derive the linear shape functions as

$$N_i(t)=1-\frac{t}{\Delta t},N_j(t)=\frac{t}{\Delta t} \tag{81}$$

Therefore, the time derivative of the temperature is thus written as

$$\frac{\partial T(t)}{\partial t}=\frac{\partial N_i(t)}{\partial t}T_i(t)+\frac{\partial N_j(t)}{\partial t}T_j(t)=\left(-\frac{1}{\Delta t}\right)T_i(t)+\left(\frac{1}{\Delta t}\right)T_j(t)=\frac{1}{\Delta t}\left(T_j(t)-T_i(t)\right)$$
$$\Rightarrow \frac{\partial T(t)}{\partial t}=\begin{bmatrix}-\frac{1}{\Delta t} & \frac{1}{\Delta t}\end{bmatrix}\begin{Bmatrix}T_i(t)\\T_j(t)\end{Bmatrix} \tag{82}$$

Substituting Equs. (77) and (79) into Equ. (54) and applying the weighted residual principle (Galerkin method), we obtain for a time interval of Δt,

$$\int_{\Delta t}\left[\begin{bmatrix}N_i(t)\\N_j(t)\end{bmatrix}\left[[\boldsymbol{C}]\begin{bmatrix}-\frac{1}{\Delta t} & \frac{1}{\Delta t}\end{bmatrix}\begin{Bmatrix}T_i(t)\\T_j(t)\end{Bmatrix}+[\boldsymbol{K}(T)]\begin{bmatrix}N_i(t) & N_j(t)\end{bmatrix}\begin{Bmatrix}T_i(t)\\T_j(t)\end{Bmatrix}-[\boldsymbol{f}(T)]\right]\right]dt \tag{83}$$

After expansion, we have

$$\int_{\Delta t}\left[\left[[\boldsymbol{C}]\begin{bmatrix}N_i(t)\\N_j(t)\end{bmatrix}\begin{bmatrix}-\frac{1}{\Delta t} & \frac{1}{\Delta t}\end{bmatrix}\begin{Bmatrix}T_i(t)\\T_j(t)\end{Bmatrix}+[\boldsymbol{K}(T)]\begin{bmatrix}N_i(t)\\N_j(t)\end{bmatrix}\begin{bmatrix}N_i(t) & N_j(t)\end{bmatrix}\begin{Bmatrix}T_i(t)\\T_j(t)\end{Bmatrix}-\begin{bmatrix}N_i(t)\\N_j(t)\end{bmatrix}[\boldsymbol{f}(T)]\right]\right]dt \tag{84}$$

Substituting Equ. (78) into Equ. (81)

$$\int_{\Delta t}\left[\left[[\boldsymbol{C}]\begin{bmatrix}1-\frac{t}{\Delta t}\\ \frac{t}{\Delta t}\end{bmatrix}\begin{bmatrix}-\frac{1}{\Delta t} & \frac{1}{\Delta t}\end{bmatrix}\begin{Bmatrix}T_i(t)\\T_j(t)\end{Bmatrix}+[\boldsymbol{K}(T)]\begin{bmatrix}1-\frac{t}{\Delta t}\\ \frac{t}{\Delta t}\end{bmatrix}\begin{bmatrix}1-\frac{t}{\Delta t} & \frac{t}{\Delta t}\end{bmatrix}\begin{Bmatrix}T_i(t)\\T_j(t)\end{Bmatrix}-\begin{bmatrix}1-\frac{t}{\Delta t}\\ \frac{t}{\Delta t}\end{bmatrix}[\boldsymbol{f}(T)]\right]\right]dt \tag{85}$$

Again, after expansion of Eq. (85), one arrives at

$$\int_{\Delta t}\left[\left[[\boldsymbol{C}]\begin{bmatrix}-\left(1-\frac{t}{\Delta t}\right)\left(\frac{1}{\Delta t}\right) & \left(1-\frac{t}{\Delta t}\right)\left(\frac{1}{\Delta t}\right)\\ -\left(\frac{t}{\Delta t}\right)\left(\frac{1}{\Delta t}\right) & \left(\frac{t}{\Delta t}\right)\left(\frac{1}{\Delta t}\right)\end{bmatrix}\begin{Bmatrix}T_i(t)\\T_j(t)\end{Bmatrix}+[\boldsymbol{K}(T)]\begin{bmatrix}\left(1-\frac{t}{\Delta t}\right)^2 & \left(1-\frac{t}{\Delta t}\right)\left(\frac{t}{\Delta t}\right)\\ \left(1-\frac{t}{\Delta t}\right)\left(\frac{t}{\Delta t}\right) & \left(\frac{t}{\Delta t}\right)^2\end{bmatrix}\begin{Bmatrix}T_i(t)\\T_j(t)\end{Bmatrix}-\begin{bmatrix}1-\frac{t}{\Delta t}\\ \frac{t}{\Delta t}\end{bmatrix}[\boldsymbol{f}(T)]\right]\right]dt \tag{86}$$

After the evaluation of Eq. (86), we obtained the characteristic equation over the time interval Δt as

$$\frac{1}{2\Delta t}\left[[\boldsymbol{C}]\begin{bmatrix}-1 & 1\\ -1 & 1\end{bmatrix}\begin{Bmatrix}T_i(t)\\T_j(t)\end{Bmatrix}+\frac{1}{3}[\boldsymbol{K}(T)]\begin{bmatrix}2 & 1\\ 1 & 2\end{bmatrix}\begin{Bmatrix}T_i(t)\\T_j(t)\end{Bmatrix}=\frac{1}{2}\begin{bmatrix}1\\1\end{bmatrix}\begin{Bmatrix}f_1\\f_2\end{Bmatrix}\right] \tag{87}$$

The above equation involves the temperature values at the mth and $(m+1)th$ level. The quadratic variation of temperature with respect to time shown in Eq. (73) can be treated in a similar fashion.

The boundary conditions and the temperature-dependent parameters are incorporated in the computer program used to solve the system of differential equations. Although, a dimensionless form of the governing equation can be derived for the computer program,

so that the handling of physical quantities is simplified. It should be noted that the thermal properties are evaluated directly in each time step from the nodal temperatures. This eliminates any iteration within each time step for the evaluations of the temperature-dependent parameters.

The element equation/matrix has been derived as shown in the previous equations. It should be noted that the whole domain was divided into a set of 50line elements. Assembling all the elements equation/matrices, a global matrix or a system of equations was obtained. After applying the boundary conditions, the resulting systems of equations is solved numerically.

The convergence criterion of the numerical solution along with error estimation has been set to

$$\sum_{i}^{N}\left|\phi_i^i - \phi^{i-1}\right| \le 10^{-4} \tag{88}$$

where φ is the general dependent variable T and i is the number of iterations.

It should be noted that a steady state is attained when $\frac{\partial T}{\partial t} = 0$ or $t \to \infty$.

Table 4: Thermo-geometric parameters used for the simulation

S/N	Parameter	Value of Parameter
1	Fin thickness (δ)	0.005 m
2	Fin length (L)	0.10 m
3	Specific heat (C)	0.048 kJ/kg^{o}C
4	Density of the fin material (ρ)	7800 kg/m^3
5	Thermal conductivity (k)	12W/m^{o}C
6	Heat transfer coefficient (h_o)	20 W/m^{2o}C
7	Electrical conductivity (σ_m)	5x10^7 S/m
8	Magnetic field intensity (B_0)	5μT
9	Axial velocity (u)	2.5 m/s
10	power-index, $p = q = r$	0.175
11	Fin base temperature (T_b)	200^{o}C
12	Initial temperature (T_o)	200^{o}C
13	Ambient temperature (T_∞)	30^{o}C
14	Time step (Δt)	10 sec

4. Results and Discussion

For the computational domain, numerical solutions are computed and the necessary convergence of the results is achieved with the desired degree of accuracy. Using the numerical solutions, parametric studies are carried out. Also, in order to define the validity of the results of thermal analysis of fin with assumed insulated tip and that of convective tip, effects of the fin tip conditions on the transient thermal response are investigated. The results with the discussion are illustrated through the Figs. 6-18 and Tables 5-6 to substantiate the applicability of the present analysis.

4.1 Verification of results

In order to verify the accuracy of the present numerical method, the numerical results are compared with results obtained by exact analytical method for the linear equation in Eq. (14) as shown in Table 5 and Fig. 6. It is inferred from the figure that there are excellent

agreements between the FEM results and the analytical results, which testifies to the validity of the FEM code. This validation boosts the confidence in the numerical outcomes of the present study. Moreover, it is observed that in the same domain by increasing the polynomial degree of approximation or the number of nodes in an element, one can achieve the desired accuracy with less DOF.

Table 5 shows the comparison of the results obtained by exact analytical and finite element methods for a conductive-convective fin with constant thermal and physical properties of fin having negligible radiation and magnetic field effects. Very good agreements are found between the exact analytical and finite element solutions. The average percentage error of the numerical solution is 0.133 %.

Table 5. Comparison of results

x(m)	Exact analytical Method (°C)	Finite Element Method (°C)	Error	% Error
0.000	200.000	200.000	0.000	0.000
0.020	148.133	148.184	0.051	0.034
0.040	113.895	114.031	0.136	0.119
0.060	92.169	92.339	0.170	0.184
0.080	79.725	79.912	0.187	0.235
0.100	74.710	74.880	0.170	0.228

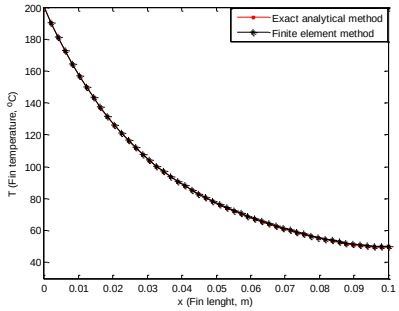

Fig. 6 Comparison of results

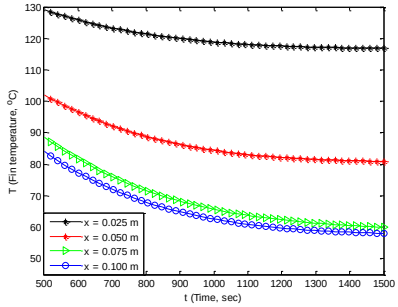

Fig. 7(a) Fin temperature profile at different location (convective tip)

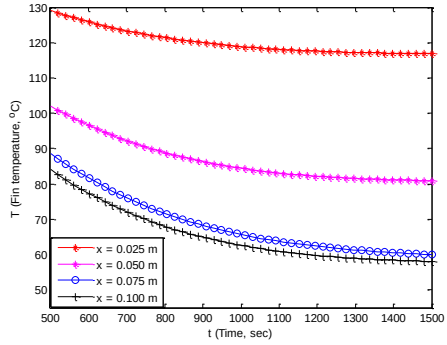

Fig. 8 Fin temperature profile at different location (insulated tip)

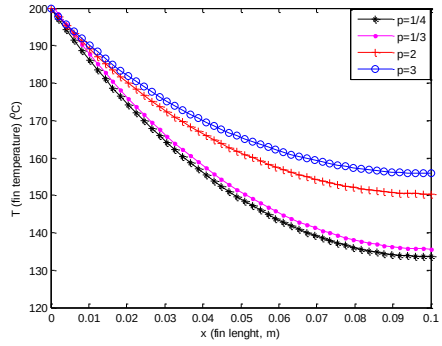

Fig. 7(b) Effects of multi-boiling parameter on the fin temperature distribution

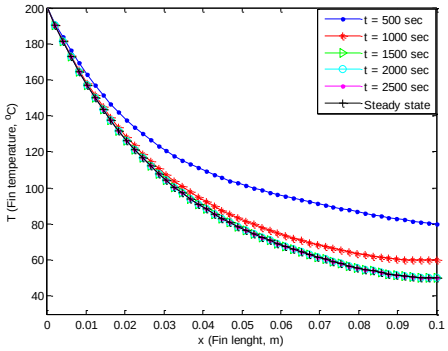

Fig. 9 Fin temperature profile at different time(convective tip)

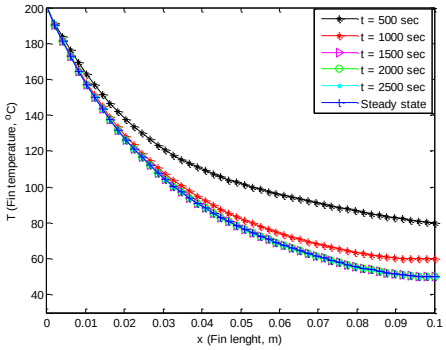

Fig. 10 Fin temperature profile at different time(convective tip)

Figs. 7 and 8 depict temperature-time history at different four points (0.025 m, 0.050m, 0.075 m and 0.100 m) of the convective-radiative fin with convective and insulated tips, respectively while Fig. 9 and 10 show the temperature profiles of the fin at difference times. The temperature histories at the four points decrease at a faster rate initially, slows down thereafter and finally tending to reach a constant value showing to be near to steady state. Also, a marginal or slightly higher temperature differences are notice between the convective and insulated tip. However, this temperature differences become appreciable as the length of the fin increases and heat is transferred within a short period of time. It could be inferred form the figures and the preceding discussion that for a short fin that undergo heat transfer for a prolonged period of time, adiabatic/insulted condition at the tip can be assumed without any significant loss in accuracy.

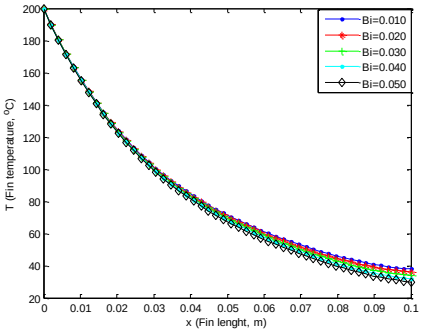

Fig. 11 Effects of Biot number on the fin temperature profile (convective-tip)

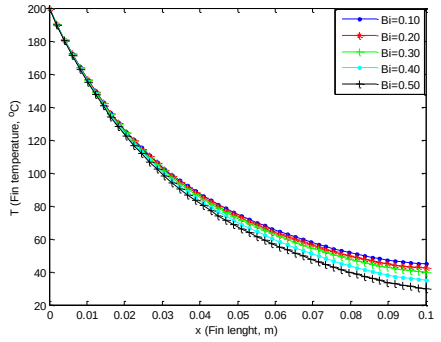

Fig. 12 Effects of Biot number on the fin temperature profile(insulated tip)

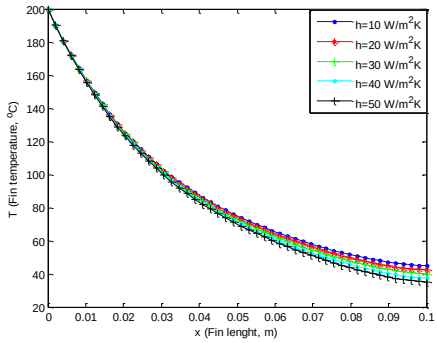

Fig. 13 Effects of heat transfer coefficient on the fin temperature profil

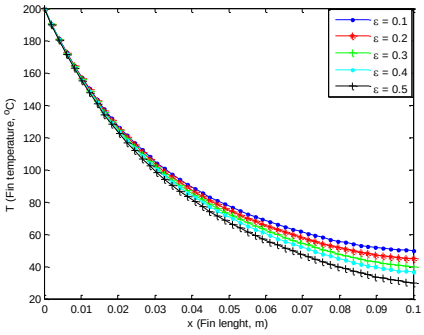

Fig. 14 Effects of emissivity on the fin temperature profile

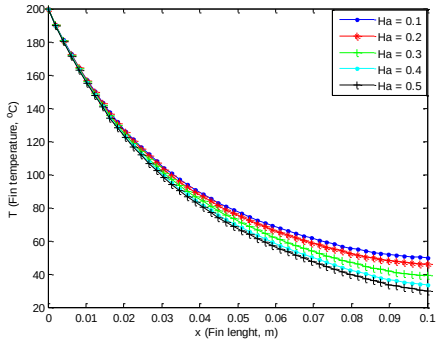

Fig. 15 Effects of magnetic parameter on the fin temperature profile

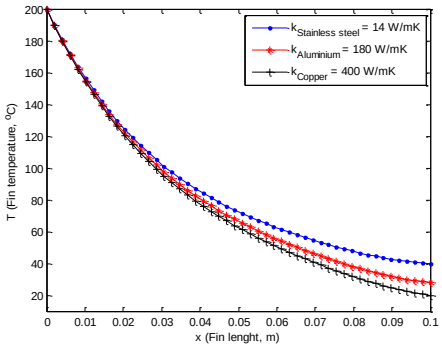

Fig. 16 Effects of thermal conductivity on the fin temperature profile

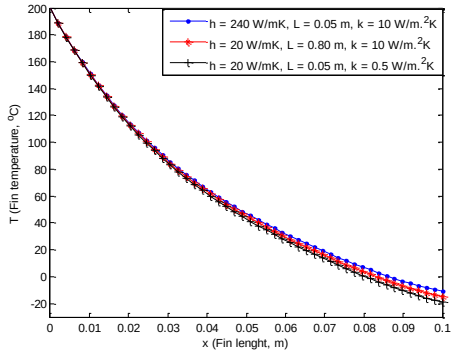

Fig. 17 Effects of thermo-geometric parameter on fin temperature profile

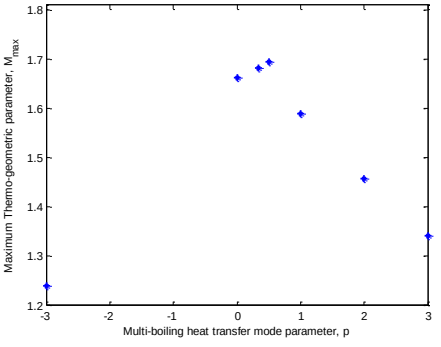

Fig. 18 Effects of multi-boiling parameter on thermal stability of the fin

It has been established that the criterion and errors due to one-dimensional heat transfer analysis is that fin base thickness Biot number should be much smaller than unity (precisely, *Bi < 0.1*). To this end, a one-dimensional analysis has been carried out and simulated within *0 < Bi <0.1*. In this case the error made in the determination of the rate of

heat transfer from the fin to the fluid surrounding it is less than 1% [67, 68]. However, when the Biot number is greater than 0.1 (Bi > 0.1), two-dimensional analysis of the fin is recommended as one-dimensional analysis predicts unreliable results for such limit.

Figs. 11 and 12 show the effects of Biot number (conduction-convection parameter) on the temperature distribution in the fin with convective and insulated tips, respectively. From the figures, it is shown that as the Biot number increases, the rate of heat transfer through the fin increases as the temperature in the fin drops faster (becomes steeper reflecting high base heat flow rates) as depicted in the figures.

Effects of heat transfer coefficient on the temperature distribution in the fin is shown in Fig.13. It is shown that the temperature profiles for the various heat transfer coefficient coincide initially but part away as we move towards the tip of the fin. This is due to the fact that coefficient of heat transfer coefficient is a factor/multiplier of the temperature difference between the fin surface and surrounding medium ($T-T_\infty$). It should be noted that the temperature difference between the fin surface and the surrounding decreases as we move away from the fin base to the fin tip even despite the increase in the heat transfer coefficient increases.

It should be noted that for the fin with heat transfer coefficient which varies according to power-law, the hypothetical boundary condition (that is, insulation) at the tip of the fin is taken into account. If the tip is not assumed to be insulated, then the problem becomes overdetermined [68]. This boundary condition is realized for sufficiently long fins. Also, it should be stated that the assumption that the heat transfer coefficient is constant yields incorrect.

Fig. 14 presents the impact of emissivity on the temperature distribution. The temperature of the fin decreases with increase of emissivity value. This is because of increase of emissive heat by radiation from the fin surface especially when the distance from the base increase. Therefore, heat transfer rate increases as the emissivity increases. The radiative eat transfer can be neglected if the base temperature of the fin is low and the emissivity of the fin surface is near zero. The important things in fins surface must be emissive because of high emissivity give a great amount of heat radiation transfer from the fin [38]. It is also established that by increasing the generation-conduction parameter and radiation-conduction parameter, the fin temperature will increase [71].

Fig.15 shows that effects of magnetic parameter, Hartman number on the temperature distribution in the porous fin. The figure depicts that the induced magnetic field in the fin can improve heat transfer through the fin. It is shown that increase in magnetic field on the fin increase the rate of heat transfer from the fin and consequently improve the efficiency of the fin. Fig. 16 shows the effect thermal conductivity of the fin materials on the thermal response of the fin. It could be inferred from the figure that more heat is transferred from fin made of copper material than the fins made of stainless steel and aluminum materials.

Effects of the thermal and geometric parameters on the temperature profile of the fin are shown in Fig. 17 while Fig. 18 shows the influence of thermo-geometric parameter ($M=(hP/kA)^{0.5}$) on the thermal stability of the fin. It was established that the value of M produces physically unsound behavior for larger values of the thermo-geometric parameter. It is shown that for growing values of the thermo-geometric parameter the temperature tends to negative values at the tip of the fin which shows thermal instability, contradicting the assumption of Eq. 9. Following the assumptions made regarding the numerical solution of the problem, it was realized that these solutions are not only physically unsound but also point toward thermal instability. Therefore, in order for the solution to be physically sound the fin thermo-geometric parameter M_{max} must not exceed a specific value. By extension, in order to ensure stability and avoid numerical diffusion of

the solution by the Galerkin finite element method, the thermo-geometric parameter, *M* must not exceed a certain value.

Table 6a. Effects of convective and insulated tip on the fin temperature distribution

Time (sec.)	Fin Temperature (°C) at x=0.025 m			Fin Temperature (°C) at x=0.050 m		
	Convective tip	**Insulated tip**	**Difference**	**Convective tip**	**Insulated tip**	**Difference**
500	129.09	129.45	0.36	102.07	103.00	0.93
1000	118.86	119.16	0.30	84.41	85.08	0.67
1500	116.84	117.04	0.20	80.84	81.31	0.47
2000	116.41	116.58	0.17	80.10	80.49	0.39
2500	116.32	116.48	0.16	79.94	80.31	0.38
∞	116.30	116.45	0.15	79.90	80.26	0.36

Table 6b. Effects of convective and insulated tip on the fin temperature distribution

Time (sec.)	Fin Temperature (°C) at x=0.075 m			Fin Temperature (°C) at x=0.100 m		
	Convective tip	**Insulated tip**	**Difference**	**Convective tip**	**Insulated tip**	**Difference**
500	90.01	91.95	1.94	84.06	87.60	3.93
1000	68.30	69.53	1.23	62.61	64.76	2.51
1500	63.85	64.74	0.89	58.23	59.84	1.61
2000	62.91	63.69	0.78	57.30	58.76	1.46
2500	62.71	63.46	0.75	57.10	58.53	1.43
∞	62.66	63.39	0.74	57.05	58.46	1.41

It is established from the results in the Tables 6a and 6b, that for a relatively short fin operating for prolonged periods of time, the results indicate that the adiabatic/hypothetical condition (or negligible heat transfer) at the tip can be assumed without any significant loss in accuracy or equality as compared to the convective boundary at the tip. This is because, for the relatively short fin operating under a steady state, the assumption of insulated tip (or negligible heat transfer at the tip) predicted almost the same results as there is no significant difference between the results of the assumed insulated tip and convective tip. Moreover, for a sharp ended fin, its performance is the same as insulated tip fin. Under such scenario, the fin tip heat convection analysis becomes meaningless due to the infinitesimally small dissipating area. However, for a long cooling fin of finite length operating in a transient state, especially for short period of time, the assumption of insulated tip produces significant different results as compared to the results of the convective tip (Table 6b). It is therefore implied that if it is assumed that no heat transfer takes place at the fin tip, the results obtained for some ranges of thermal and geometric parameters indicate that the determination of temperature distribution and the rate of heat transfer from the fin to its surroundings includes a fairly large error for some conditions which are important for practical applications. Therefore, for transient thermal studies of fins, the assumption of no heat transfer takes place at the fin tip should be taken with caution in thermal analysis of a long cooling fin of finite length operating within a short period of time such as the fin operating under picosecond or nanosecond. Also, such an assumption should not be made when the convective heat transfer coefficient at the tip of the fin is very high or the thermal conductivity of the fin material is very low. It was established that the difference between the results of the insulated tip and convective tip increases as the tip Biot number is increased. In fact, the percentage error of the difference between the results of the insulated tip and convective tip for a very high value of heat transfer coefficient could be as high as 20 % [72].

5. Conclusion

In this work, transient thermal behavior of convective-radiative cooling fin with convective tip and subjected to magnetic field have been analyzed using Galerkin finite element method. The numerical solutions are verified by the exact solution developed using Laplace transform. The study revealed that increase in Biot number, convective, radiative and magnetic parameters increase the rate of heat transfer from the fin and consequently, improved the efficiency of the fin. Also, it was established that for a relatively short fin operating for prolonged periods of time or steady state, the adiabatic/hypothetical condition (or negligible heat transfer) at the tip can be assumed without any significant loss in accuracy or equality as compared to the convective condition at the tip. However, for a long cooling fin of finite length operating in a transient state, especially for short period of time, the assumption of insulated tip produces significant different results as compared to the results of the convective tip. Therefore, for transient thermal studies of fins, the assumption that no heat transfer takes place at the fin tip should be taken with caution for a long cooling fin of finite length operating within a relatively short period of time. It is hope that the present study will enhance the understanding of thermal response of solid fin under various factors and especially of practical significance in chemical and nuclear engineering.

Nomenclature

A cross sectional area of the fins, m^2

B_o Magnetic field intensity (T)

Bi Biot number

C_p specific heat ($J\ kg^{-1}\ K^{-1}$)

H Heat transfer coefficient ($Jm^{-2}\ K^{-1}$)

h_b heat transfer coefficient at the base of the fin, ($Wm^{-2}k^{-1}$)

J Total current intensity (A)

J_c Conduction current intensity (A)

k thermal conductivity of the fin material, ($Wm^{-1}k^{-1}$)

k_b thermal conductivity of the fin material at the base, ($Wm^{-1}k^{-1}$)

L Length of the fin (m)

M dimensionless thermo-geometric parameter

P perimeter of the fin(m)

q heat transfer rate W

t time

T fin temperature (K)

T_∞ ambient temperature, K

T_b Temperature at the base of the fin, K

w width of the fin

x axial length measured from fin base (m)

w width of the fin

Greek Symbols

ε Emissivity

σ Electric conductivity (A/m)

σ_{st} Stefan–Boltzmann constant ($Wm^2 K^4$)

ρ Density of the fluid (kgm^{-3})

β thermal conductivity parameter

δ thickness of the fin, m

References

[1] P. Y. Wang P.Y., G. C. Kuo, Y. H. Hu, W. L. Liaw. Transient temperature solutions of a cylindrical fin with lateral heat loss, Wseas Transactions on Mathematics, 11(10) (2012), 918-925.

[2] R. J. Moitsheki, C. Harley. Transient heat transfer in longitudinal fins of various profiles with temperature-dependent thermal conductivity and heat transfer coefficient, PRAMANA, 77(3) (2011), 519–532. https://doi.org/10.1007/s12043-011-0172-6

[3] M. D. Mhlongo, R. J. Moitsheki. Some exact solutions of nonlinear fin problem for steady heat transfer in longitudinal fin with different profiles, Advances in Mathematical Physics, 2014, 1-16. https://doi.org/10.1155/2014/947160

[4] S. A. Ali, A. H. Bokhari, F. D. Zaman. A Lie symmetry classification of a nonlinear fin equation in cylindrical coordinates, Abstract and Applied Analysis, 2014, 1-10. https://doi.org/10.1155/2014/527410

[5] A.H.A Kader, M.S.A. Latif and H. M. Nour. General exact solution of the fin problem with variable thermal conductivity, Propulsion and Power Research, 5(1))2016), 63-69.

[6] R. J. Moitsheki and A. Rowjee. Steady heat transfer through a two- dimensional rectangular straight fin, Mathematical Problems in Engineering, 2011, 1-13. https://doi.org/10.1155/2011/826819

[7] K.D. Cole, Computer programs for temperature in fins and slab bodies with the method of Green's functions, Comput. Appl. Eng. Educ. 12 (3) (2004) 189–197. https://doi.org/10.1002/cae.20010

[8] A. Jordan, S. Khaldi, M. Benmouna, A. Borucki. Study of non-linear heat transfer problems, Revue Phys. Appl., 22(1987),101-105. https://doi.org/10.1051/rphysap:01987002201010100

[9] B. Kundu, P.K. Das. Performance analysis and optimization of straight taper fins with variable heat transfer coefficient, International Journal of Heat and Mass Transfer, 45(2002), 4739- 4751. https://doi.org/10.1016/S0017-9310(02)00189-8

[10] F. Khani, M. A. Raji, H. H. Nejad. Analytical solutions and efficiency of the nonlinear fin problem with temperature-dependent thermal conductivity and heat transfer coefficient, Commun Nonlinear Sci Numer Simulat, 14(2009), 3327-3338. https://doi.org/10.1016/j.cnsns.2009.01.012

[11] S. R. Amirkolei and D. D. Ganji D.D. Thermal performance of a trapezoidal and rectangular profiles fin with temperature-dependent heat transfer coefficient, thermal conductivity and emissivity, Indian J. Sci. Res., 1(2)(2014), 223-229.

[12] A. Aziz, M. N. Bouaziz. A least squares method for a longitudinal fin with temperature dependent internal heat generation and thermal conductivity, Energy Conversion and Management, 52(2011), 2876-2882.https://doi.org/10.1016/j.enconman.2011.04.003

[13] M. G. Sobamowo. Thermal analysis of longitudinal fin with temperature dependent properties and internal heat generation using Galerkin's method of weighted residual, Applied Thermal Engineering, 99(2016), 1316-1330. https://doi.org/10.1016/j.applthermaleng.2015.11.076

[14] D. D. Ganji, M. Raghoshay, M. Rahimi, M. Jafari. Numerical investigation of fin efficiency and temperature distribution of conductive, convective and radiative straight fins, IJRRAS, 2010, 230-237.

[15]. M. G. Sobamowo, O. M. Kamiyo and O. A. Adeleye. Thermal performance analysis of a natural convection porous fin with temperature-dependent thermal conductivity and internal heat generation. Thermal Science and Engineering Progress. 1(2017) 39-52. https://doi.org/10.1016/j.tsep.2017.02.007

[16] M. G. Sobamowo. Thermal performance and optimum design analysis of fin with variable thermal conductivity using double decomposition method. Journal of Mechanical Engineering and Technology. Vol. 9(1), 1-32.

[17] M. G. Sobamowo, L. O. Jayesimi and J. D. Femi-Oyetoro (2017). Heat transfer study in a convective-radiative fin with temperature-dependent thermal conductivity and magnetic field using variation of parameter method. Journal of Applied Mathematics and Computational Mechanics, 16(3), 85-96. https://doi.org/10.17512/jamcm.2017.3.08

[18] A. Moradi and H. Ahmadikia. Analytical solution for different profiles of fin with temperature dependent thermal conductivity, Mathematical Problems in Engineering, 2010, 1-15. https://doi.org/10.1155/2010/568263

[19] S. Sadri, M. R. Raveshi and S. Amiri. Efficiency analysis of straight fin with variable heat transfer coefficient and thermal conductivity, Journal of Mechanical Science and Technology, 26(4)(2011), 1283-1290. https://doi.org/10.1007/s12206-012-0202-4

[20] P. L. Ndlovu and R. J. Moitsheki. Analytical solutions for steady heat transfer in longitudinal fins with temperature dependent properties, Mathematical Problems in Engineering, 2013, 1-14. https://doi.org/10.1155/2013/273052

[21] S. Mosayebidorcheh, D. D. Ganji, M. Farzinpoor. Approximate solution of the nonlinear heat transfer equation of a fin with the power-law temperature- dependent thermal conductivity and heat transfer coefficient, Propulsion and Power Research, 3(1)(2014), 41-47. https://doi.org/10.1016/j.jppr.2014.01.005

[22] S. E. Ghasemi, M. Hatami, D. D. Ganji. Thermal analysis of convective fin with temperature-dependent thermal conductivity and heat generation, Case Studies in Thermal Engineering, 4(2014), 1-8. https://doi.org/10.1016/j.csite.2014.05.002

[23] D. D. Ganji and A.S. Dogonchi. Analytical investigation of convective heat transfer of a longitudinal fin with temperature- dependent thermal conductivity, heat transfer coefficient and heat generation, International Journal of Physical Sciences, 9(21) (2014), 466-474.

[24] M. G. Sobamowo, O. A. Adeleye and A. A. Yinusa. Analysis of convective-radiative porous fin with temperature-dependent internal heat generation and magnetic using homotopy perturbation method. Journal of computational and Applied Mechanics. Vol. 12(2)(2017), 127-145.

[25] C. Arslanturk. Optimization of straight fins with step change in thickness and variable thermal conductivity by homotopy perturbation method, J. of Thermal Science and Technology, 10(2010), 9-19.

[26] D. D. Ganji, Z. Z. Ganji, H. D. Ganji (2011). Determination of temperature distribution for annular fins with temperature dependent thermal conductivity by HPM, Thermal Science, Vol. 15(1)(2011), 111-115.

[27] H. A. Hoshyar, I. Rahimipetroudi, D. D. Ganji, A. R. Majidian. Thermal performance of porous fins with temperature-dependent heat generation via the homotopy perturbation method and collocation method, Journal of Applied Mathematics and Computational Mechanics, Vol. 14(4)(2015), 53-65. https://doi.org/10.17512/jamcm.2015.4.

[28] I.V. Singh, K. Sandeep, R. Prakash. Heat transfer analysis of two-dimensional fins using a meshless element free Galerkin method, Numerical Heat Transfer, Part A, 44(2003), 73-84. https://doi.org/10.1080/713838174

[29] S. Basri, M. M. Fakir, F. Mustapha, D. L. A. Majid, A. A. Jaafar. Heat distribution in rectangular fins using efficient finite element and differential quadrature methods, Engineering, 1(2009), 151-160. https://doi.org/10.4236/eng.2009.13018

[30] T. Singh, S. Shrivastava, H. S. Ber H.S. Analysis of unsteady heat conduction through short fin with applicability of quasi theory, Int. J. Mech. Eng. & Rob. Res., 2(1) (2013), 269-283.

[31] A. K. Sao, Y. P. Banjare. Analysis of thermal characteristics of transient heat conduction through long fin and comparison with exact fin theory and quasi steady theory, International Journal of Emerging Technology and Advanced Engineering. 4(11)2014, 157-166.

[32] B. Lotfi, A. Belkacem. Numerical method for optimum performance of fin profiles, International Journal of Current Engineering and Technology, 4(6)(2014), 3990-3998.

[33] A. A. A. A. Al-Rashed, L. Kolsi, H. F. Oztop, N. Abu- Hamdeh, M. N. Borjini. Natural convection and entropy production in a cubic cavity heated via pin- fins heat sinks, International Journal of Heat and Technology, 35(1)(2017), 109-115.https://doi.org/10.18280/ijht.350115

[34] D. Taler, J. Taler. Steady-state and transient heat transfer through fins of complex geometry, Archives of Thermodynamics, 35(2)(2014),117-133. https://doi.org/10.2478/aoter-2014-0017

[35] P. Malekzadeh and H. Rahideh. Two-dimensional nonlinear transient heat transfer analysis of variable section pin fins, Energy Conversion and Management, 50(2009), 916-922. https://doi.org/10.1016/j.enconman.2008.12.025

[36] C. S. Reddy, Y. R. Reddy, P. Srikanth. Application of B–spline based FEM to one-dimensional problems, International Journal of Current Engineering and Technology, 3(2014), 137-140.

[37] Y. Sun, J. Ma, B. Li, Z. Guo. Prediction of nonlinear heat transfer in a convective radiative fin with temperature-dependent properties by the collocation spectral method, Numerical Heat Transfer, Part B: Fundamentals, 69(1), (2016), 8-73. https://doi.org/10.1080/10407782.2015.1081043

[38] G. Rajul, T. Harishchandra, T. Brajesh. Nonlinear numerical analysis of convective-radiative fin using MLPG method. International journal of heat and technology, 35(4)(2017), 721-729

[39] Z. Wei, L. Haifang, D. Xiaoze, Y. Yongping, S. Lei. Numerical and experimental research on performance of single- row finned tubes in air-cooled power plants, International Journal of Heat and Technology, 34(1)(2016), 137-142. https://doi.org/10.18280/ijht.340120

[40] F. Hajabdollahi, H. H. Rafsanjani, Z. Hajabdollahi, Y. Hamidi. Multi- objective optimization of pin fin to determine the optimal fin geometry using genetic algorithm, Applied Mathematical Modelling, 36(2012), 244-254. https://doi.org/10.1016/j.apm.2011.05.048

[41] H. Fatoorehchi, H. Abolghasemi. Investigation of nonlinear problems of heat conduction in tapered cooling fins via symbolic programming, Appl. Appl. Math., 7(2)(2012), 717-734.

[42] M. S. A. Latif, A. H. A Kader, H. M. Nour. Exact implicit solution of nonlinear heat transfer in rectangular straight fin using symmetry reduction methods, Appl. Appl. Math., 10(2)(2015), 864-877.

[43] A. Mahmoudi, I. Mejri. Analysis of conduction radiation heat transfer with variable thermal conductivity and variable refractive index: Application of the Lattice Boltzmann method, International Journal of Heat and Technology, 33(1)(2015), 1- 8. https://doi.org/10.18280/ijht.330101

[44]. M. G. Sobamowo. Analysis of longitudinal fin with temperature-dependent thermal conductivity and internal heat generation. Alexandra Engineering Journal, 56(2017), 1-11. https://doi.org/10.1016/j.aej.2016.04.022

[45]. M. G. Sobamowo, B. Y. Ogumola and G. Nzebuka. Finite volume method for analysis of convective longitudinal fin with temperature-dependent thermal conductivity and internal heat generation. Tranfer Phenoma in Fluid and Heat Flows III. Defect and Diffusin Forum. 374(2017), 106-120.

[46] M. G. Sobamowo, G. A. Oguntala and J. D. Femi-Oyetoro. Investigation of the effects of magnetic field on the thermal performance of convective-radiative fin using wavelet collocation method. Annals of Faculty of Engineering Honedoara-International Journal of Engineering. Tome XV(2017), 179-186.

[47] M. G. Sobamowo. Heat transfer study in porous fin with temperature-dependent thermal conductivity and internal heat generation using Legendre wavelet collocation method. Communication in Mathematical Modeling and Applications. Vol. 2(3)(2017), 16-28.

[48] M. G. Sobamowo and O. M. Kamiyo. Multi-boiling heat transfer analysis of a convective straight fin with temperature-dependent thermal properties and internal heat generation. Journal of Applied and Computational Mechanics. 3(4)(2017), 229-239.

[49] M. G. Sobamowo. Analysis of heat transfer in porous fin with temperature-dependent thermal conductivity and internal heat generation using Chebychev spectral collocation method. Journal of Computational Applied Mechanics. Vol. 48(2) (2017), 271-287.

[50] A.J. Chapman, Transient heat conduction in annular fins of uniform thickness, Chem. Eng. Symp. 55(29), (1959) 195–201.

[51] A.B. Donaldson, A.R. Shouman, Unsteady-state temperature distribution in a convecting fin of constant area, Appl. Sci. Res. 26 (1–2)(1972), 75– 85. https://doi.org/10.1007/BF01897836

[52] N.V. Suryanarayana, Transient response of straight fins, J. Heat Transf. 97 (1975), 417–423. https://doi.org/10.1115/1.3450391

[53] N.V. Suryanarayana, Transient response of straight fins part II, J. Heat Transf. 98 (1976), 324–326. https://doi.org/10.1115/1.3450546

[54] J. Mao, S. Rooke, Transient analysis of extended surfaces with convective tip, Int. Commun. Heat Mass Transf. 21 (1994), 85–94. https://doi.org/10.1016/0735-1933(94)90086-8

[55] J.V. Beck, K.D. Cole, A. Haji-Sheikh, B. Litkouhi, Heat Conduction Using Green's Functions Hemisphere, New York, 1992.

[56] R.H. Kim, The Kantorovich method in the variational formulation to an unsteady heat conduction. Lett. Heat Mass Transf. 3 (1) (1976), 73–80.

[57] A. Aziz, T.Y. Na, Transient response of fins by coordinate perturbation expansion, Int. J. He- at and Mass Transfer 23 (1980),1695–1698. https://doi.org/10.1016/0017-9310(80)90232-X

[58] A. Aziz, A.D. Kraus, Transient heat transfer in extended surfaces, Appl. Mech. Rev. 48 (3) (1995), 317–349. https://doi.org/10.1115/1.3005105

[59] A. Campo and A. Salazar, Similarity between unsteady-state conduction in a planar slab for short times and steady-state conduction in a uniform, straight fin, Heat Mass Transf. 31 (5) (1996), 365–370. https://doi.org/10.1007/BF02184052

[60] A.K. Saha, S. Acharya, Parametric study of unsteady flow and heat transfer in a pin-fin heat exchanger, Int. J. Heat Mass Transf. 46 (20) (2003), 3815–3830. https://doi.org/10.1016/S0017-9310(03)00190-X

[61] T.H. Hsu, C.K. Chen, Transient analysis of combined forced and free convection conduction along a vertical circular fin in micro polar fluids, Numer. Heat Transf. A 19 (2) (1991), 177–185. https://doi.org/10.1080/10407789108944844

[62] M. Benmadda, M. Lacroix, Transient natural convection from a finned surface for thermal storage in an enclosure, Numer. Heat Transf. A 29 (1) (1996), 103– 114. https://doi.org/10.1080/10407789608913781

[63] D.K. Tafti, L.W. Zhang, G. Wang, Time-dependent calculation procedure for fully developed and developing flow and heat transfer in louvered fin geometries, Numer. Heat Transf. A 35 (3) (1999), 225–249. https://doi.org/10.1080/104077899275227

[64] A.K. Saha, S. Acharya, Unsteady simulation of turbulent flow and heat transfer in a channel with periodic array of cubic pin-fins, Numer. Heat Transf. A 46 (8) (2004), 731–763 Exact Solution for Transient Heat Conduction through Long Fin. https://doi.org/10.1080/104077890504465

[65] M. Tutar, A. Akkoca, Numerical analysis of fluid flow and heat transfer characteristics in three-dimensional plate fin-and-tube heat exchangers, Numer. Heat Transf. A 46 (3) (2004), 301–321. https://doi.org/10.1080/10407780490474762

[66] I. Mutlu, T.T. Al-Shemmeri, Steady-state and transient performance of a shrouded Longitudinal fin array, Int. Commun. Heat Mass Transf. 20 (1993), 133–143. https://doi.org/10.1016/0735-1933(93)90014-M

[67] R. K. Irey, Errors in the one-dimensional fin solution, J. Heat Transfer 90, 175 176 (1968).

[68] K Laor and H Kalman. The effect of tip convection on the performance and optimum dimension of cooling fins. Int. Comm. Heat Mass Transfer, 19(1992), 569-584.https://doi.org/10.1016/0735-1933(92)90012-7

[69] W. Lau and C. W. Tan, Errors in one-dimensional heat transfer analysis in straight and annular fins, J. Heat Transfer 95(1973), 549-551.https://doi.org/10.1115/1.3450110

[70] H. C. Unal, Determination of the temperature distribution in an extended surface with a non-uniform heat Effect of the boundary condition at a fin tip on the performance of the fin

1495 transfer coefficient, Int. J. Heat Mass Transfer 28(1985), 2279-2284. https://doi.org/10.1016/0017-9310(85)90046-8

[71] S.A. Atouei, Kh. Hosseinzadeh, M. Hatami, Seiyed E. Ghasemi, D.D. Ganji. Heat transfer study on convective–radiative semi-spherical fins with temperature-dependent properties and heat generation using efficient computational methods. Applied Thermal Engineering, Volume 89(5), 299-305, 2015. https://doi.org/10.1016/j.applthermaleng.2015.05.084

[72] M. G. Sobamowo and A. A. Oyediran. Effects of Thermo-geometric parameter on the heat transfer rate in Straight fin wit variable thermal conductivity. A Festschrift Celebrating 70 years of Life and Excellence of Emeritus Professor Vincent Olusegun Sowemimo Olunloyo, 2013.